

Curvature and geodesic instabilities in a geometrical approach to the planar three-body problem

GOVIND S. KRISHNASWAMI AND HIMALAYA SENAPATI

Physics Department, Chennai Mathematical Institute, SIPCOT IT Park, Siruseri 603103, India
Email: govind@cmi.ac.in, himalay@cmi.ac.in

Oct 8, 2016

Published in J. Math. Phys. 57, 102901 (2016)

Abstract

The Maupertuis principle allows us to regard classical trajectories as reparametrized geodesics of the Jacobi-Maupertuis (JM) metric on configuration space. We study this geodesic reformulation of the *planar* three-body problem with both Newtonian and attractive inverse-square potentials. The associated JM metrics possess translation and rotation isometries in addition to scaling isometries for the inverse-square potential with zero energy E . The geodesic flow on the *full* configuration space \mathbb{C}^3 (with collision points excluded) leads to corresponding flows on its Riemannian quotients: the center of mass configuration space \mathbb{C}^2 and shape space \mathbb{R}^3 (as well as \mathbb{S}^3 and the shape sphere \mathbb{S}^2 for the inverse-square potential when $E = 0$). The corresponding Riemannian submersions are described explicitly in ‘Hopf’ coordinates which are particularly adapted to the isometries. For equal masses subject to inverse-square potentials, Montgomery shows that the zero-energy ‘pair of pants’ JM metric on the shape sphere is geodesically complete and has negative gaussian curvature except at Lagrange points. We extend this to a proof of boundedness and strict negativity of scalar curvatures everywhere on \mathbb{C}^2 , \mathbb{R}^3 and \mathbb{S}^3 with collision points removed. Sectional curvatures are also found to be largely negative, indicating widespread geodesic instabilities. We obtain asymptotic metrics near collisions, show that scalar curvatures have finite limits and observe that the geodesic reformulation ‘regularizes’ pairwise and triple collisions on \mathbb{C}^2 and its quotients for arbitrary masses and allowed energies. For the Newtonian potential with equal masses and zero energy, we find that the scalar curvature on \mathbb{C}^2 is strictly negative though it could have either sign on \mathbb{R}^3 . However, unlike for the inverse-square potential, geodesics can encounter curvature singularities at collisions in finite geodesic time.

Keywords: Three body problem, Jacobi-Maupertuis pair of pants metric, geodesic instabilities, regularization of collisions.

Contents

1	Introduction	2
2	Trajectories as geodesics of the Jacobi-Maupertuis metric	4
3	Planar three-body problem with inverse-square potential	5
3.1	Jacobi-Maupertuis metric on configuration space and Hopf coordinates	5
3.2	Quotient JM metrics on shape space, the three-sphere and the shape sphere	9
3.3	JM metric in the near-collision limit and its completeness	11
3.3.1	Geometry near pairwise collisions	11
3.3.2	Geometry on \mathbb{R}^3 and \mathbb{C}^2 near triple collisions	13
3.4	Scalar curvature for equal masses and zero energy	14
3.5	Sectional curvature for three equal masses	17
3.6	Stability tensor and linear stability of geodesics	19
4	Planar three-body problem with Newtonian potential	21
4.1	JM metric and its curvature on configuration and shape space	21
4.2	Near-collision geometry and ‘geodesic incompleteness’	22
A	Proof of an inequality to give an upper bound for the scalar curvature	23

1 Introduction

The classical three-body problem and associated questions of stability have stimulated much work in mechanics and nonlinear & chaotic dynamics [1, 2, 3, 4, 5]. Quantum and fluid mechanical variants with potentials other than Newtonian are also of interest: e.g., the dynamics of two-electron atoms and the water molecule [6], the N -vortex problem with logarithmic potentials [7], the problem of three identical bosons with inverse-square potentials (Efimov effect in cold atoms [8, 9]) and the Calogero-Moser system also with inverse-square potentials [10]. We investigate a geometrical approach to the planar three-body problem with Newtonian and attractive inverse-square potentials. The inverse-square potential has some simplifying features over the Newtonian one due in part to the nature of its scaling symmetry $H(\lambda \mathbf{r}, \lambda^{-1} \mathbf{p}) = \lambda^{-2} H(\mathbf{r}, \mathbf{p})$. As a consequence, the sign of energy E controls asymptotic behaviour: bodies fly apart or suffer a triple collision according as E is positive/negative, leaving open the special case $E = 0$ [11]. This follows from the Lagrange-Jacobi identity $\ddot{I} = 4E$ for the evolution of the moment of inertia $I = \sum m_i \mathbf{r}_i^2$. By contrast, for the Newtonian potential, $H(\lambda^{-2/3} \mathbf{r}, \lambda^{1/3} \mathbf{p}) = \lambda^{2/3} H(\mathbf{r}, \mathbf{p})$ leads to $\ddot{I} = 4E - 2V$, which is not sufficient to determine the long time behavior of I when $E < 0$.

Our approach is based on a geometric reformulation of Newtonian trajectories. It is well known that trajectories of a free particle moving on a Riemannian manifold are geodesics of a mass/kinetic metric m_{ij} defined by the kinetic energy $\frac{1}{2} m_{ij}(x) \dot{x}^i \dot{x}^j$. Indeed, geodesic flow on a compact Riemann surface of constant negative curvature is a prototypical model for chaos [6]. In the presence of a potential V , trajectories are reparametrized geodesics of the conformally related Jacobi-Maupertuis (JM) metric $g_{ij} = (E - V(x)) m_{ij}$ (see Refs.[12, 13] and §2). The linear stability of geodesics to perturbations is then controlled by sectional curvatures of the JM

metric.

Several authors have tried to relate the geometry of the JM metric to chaos. For systems with many degrees of freedom, Pettini et. al. [14, 15, 16] obtain an approximate expression for the largest Lyapunov exponent in terms of curvatures. In Ref. [17] the geometric framework is applied to investigate chaos in the Hénon-Heiles system and a suitable average sectional curvature proposed as an indicator of chaos for systems with few degrees of freedom (see also [18]). While negativity of curvature need not imply chaos, as the Kepler problem shows for $E > 0$, these works suggest that chaos could arise both from negativity of curvature and from fluctuations in curvature through parametric instabilities.

For the *planar* gravitational three-body problem (i.e. with pairwise Newtonian potentials), the JM metric on the full configuration space $\mathbb{R}^6 \cong \mathbb{C}^3$ has isometries corresponding to translation and rotation invariance groups \mathbf{C} and $U(1)$ (§3.1). This allows one to study the reduced dynamics on the quotients: configuration space $\mathbb{C}^2 \cong \mathbb{C}^3/\mathbf{C}$ and shape space $\mathbb{R}^3 \cong \mathbb{C}^2/U(1)$ [19]. Here, collision configurations are excluded from \mathbb{C}^3 and its quotients. When the Newtonian potential is replaced with the inverse-square potential, the zero-energy JM metric acquires a scaling isometry leading to additional quotients: $\mathbb{S}^3 \cong \mathbb{C}^2/\text{scaling}$ and the shape sphere $\mathbb{S}^2 \cong \mathbb{R}^3/\text{scaling}$ (see Fig. 1c). Since the three collision points have been removed, the (non-compact) shape sphere \mathbb{S}^2 has the topology of a pair of pants and fundamental group given by the free group on two generators. As part of a series of works on the planar three-body problem, Montgomery [20] shows that for three equal masses with inverse-square potentials (sometimes referred to as a ‘strong’ force), the curvature of the JM metric on \mathbb{S}^2 is negative except at the two Lagrange points, where it vanishes. As a corollary, he shows the uniqueness of the ‘figure 8’ solution and establishes that collision solutions are dense within bound ones. In Ref. [21, 22], he uses the geometry of the shape sphere to show that zero angular momentum negative energy solutions (other than the Lagrange homotheties) of the gravitational three-body problem have at least one syzygy (collinearity).

In this paper, we begin by extending some of Montgomery’s results on the geometry of the shape sphere to that of the configuration space \mathbb{C}^2 (without any restriction on angular momentum) and its quotients. Metrics on the quotients are obtained explicitly via Riemannian submersions (§3.2, §4.1) which simplify in ‘Hopf’ coordinates, as the Killing vector fields (KVF’s) point along coordinate vector fields. These coordinates also facilitate our explicit computation of metrics and curvatures near binary and triple collisions. We interpret Lagrange and Euler homotheties (‘central configurations’ [23]) as radial geodesics at global and local minima of the conformal factor in the JM metric for the inverse-square potential (§3.3) and thereby deduce geodesic completeness of the configuration manifold \mathbb{C}^2 and its quotients \mathbb{R}^3 and \mathbb{S}^3 for arbitrary masses and allowed energies. The estimates showing completeness on \mathbb{C}^2 are similar to those showing that the classical action (integral of Lagrangian) diverges for collisional trajectories. In a private communication, R. Montgomery points out that this was known to Poincaré and has been rediscovered several times (see for example Ref. [24, 25, 26]). Completeness establishes that the geodesic reformulation ‘regularizes’ pairwise and triple collisions by reparametrizing time so that any collision occurs at $t = \infty$. In contrast with other regularizations [27, 28], this does not involve an extrapolation of the dynamics past a collision nor a change in dependent variables. Unlike for the inverse-square potential, we show that geodesics for the Newtonian potential can reach curvature singularities (binary/triple collisions) in finite geodesic time (§4.2). This may come as a surprise, since the Newtonian potential is *less* singular than the inverse-square

potential and masses collide sooner under Newtonian evolution in the inverse-square potential. However, due to the reparametrization of time in going from trajectories to geodesics, masses can collide in finite time in the Newtonian potential while taking infinitely long to do so in the inverse-square potential. Indeed, for the attractive $1/r^n$ potential, the JM line-element leads to estimates $\propto \int_0^{\eta_0} \frac{d\eta}{\eta^{n/2}}$ and $\int_0^{r_0} \frac{dr}{r^{n/2}}$ for the distances to binary and triple collisions from a nearby location (§3.3). These diverge for $n \geq 2$ and are finite for $n < 2$.

To examine stability of geodesics, we evaluate scalar and sectional curvatures of the zero-energy, equal-mass JM metrics on \mathbb{C}^2 and its quotients. For the inverse-square potential, we obtain strictly negative upper bounds for scalar curvatures on \mathbb{C}^2 , \mathbb{R}^3 and \mathbb{S}^3 (§3.4), indicating widespread linear geodesic instability. Moreover, scalar curvatures are shown to be bounded below. In particular, they remain finite and negative at binary and triple collisions. O’Neill’s theorem is used to determine or bound various sectional curvatures on \mathbb{C}^2 using the more easily determined ones on its Riemannian quotients; they are found to be largely negative (§3.5). On the other hand, for the Newtonian potential, we find that the scalar curvature on \mathbb{C}^2 is strictly negative, though it can have either sign on shape space \mathbb{R}^3 (§4.1). Unlike for the inverse-square potential, scalar curvatures $\rightarrow -\infty$ at collision points. We also discuss the geodesic instability of Lagrange rotation and homothety solutions for equal masses (§3.6). We end with a cautionary remark comparing stability of geodesics to that of corresponding trajectories, simple examples are used to illustrate that the two notions of stability need not always coincide. In this paper we have not touched upon the interesting issues of long-term geodesic stability or chaos. It would be interesting to relate the local geodesic instabilities discussed here to medium- and long-time behavior. The dynamical consequences of sectional curvatures possessing either sign should also be of much interest.

2 Trajectories as geodesics of the Jacobi-Maupertuis metric

For a system with configuration space M and Lagrangian $L = (1/2)m_{ij}(x)\dot{x}^i\dot{x}^j$, Lagrange’s equations are equivalent to the geodesic equations with respect to the ‘mass’ or ‘kinetic metric’ m_{ij} . Remarkably, this connection between trajectories and geodesics extends to a system subject to a potential V . Indeed, this is the content of Maupertuis’ principle of extremization of $\int_{q_1}^{q_2} pdq$ holding energy fixed[12, 13]. More precisely, the equations of motion (EOM)

$$m_{ki}\ddot{x}^i(t) = -\partial_k V - \frac{1}{2}(m_{ik,j} + m_{jk,i} - m_{ij,k})\dot{x}^i(t)\dot{x}^j(t) \quad (1)$$

may be regarded as reparametrized geodesic equations for the JM metric,

$$ds^2 = g_{ij}dx^i dx^j = (E - V)m_{ij}dx^i dx^j \quad (2)$$

on the classically allowed ‘Hill’ region $E - V \geq 0$. Notice that $\sqrt{2} \int ds = \int pdq = \int (L + E)dt$ so that the length of a geodesic is related to the classical action of the trajectory. The formula for the inverse JM metric $g^{ij} = m^{ij}/(E - V)$ may also be read off from the time-independent Hamilton-Jacobi (HJ) equation $(m^{ij}/2(E - V))\partial_i W \partial_j W = 1$ by analogy with the rescaled kinetic metric $m^{ij}/2E$ appearing in the free particle HJ equation $(m^{ij}/2E)\partial_i W \partial_j W = 1$ (see p.74 of Ref. [11]). The JM metric is conformal to the kinetic metric and depends parametrically on the conserved energy $E = \frac{1}{2}m_{ij}\dot{x}^i\dot{x}^j + V$. The geodesic equations

$$\ddot{x}^l(\lambda) = -\frac{1}{2}g^{lk}(g_{ki,j} + g_{kj,i} - g_{ij,k})\dot{x}^i(\lambda)\dot{x}^j(\lambda) \quad (3)$$

for the JM metric reduce to (1) under the reparametrisation $d/d\lambda = (1/\sigma)(d/dt)$ where $\sigma = (E - V)/\sqrt{\mathcal{T}}$. Here $\mathcal{T} = \frac{1}{2}g_{ij}\dot{x}^i\dot{x}^j$ is the conserved ‘kinetic energy’ along geodesics and equals one-half for arc-length parametrization. To obtain σ , suppose $y^i(t)$ is a trajectory and $z^i(\lambda)$ the corresponding geodesic. Then at a point $x^i = z^i(\lambda) = y^i(t)$, the velocities are related by $\sigma\dot{z}^i = \dot{y}^i$ leading to

$$\mathcal{T} = \frac{1}{2}g_{ij}\dot{z}^i\dot{z}^j = \frac{E - V}{2}m_{ij}\dot{z}^i\dot{z}^j = \frac{E - V}{2\sigma^2}m_{ij}\dot{y}^i\dot{y}^j = \left(\frac{E - V}{\sigma}\right)^2. \quad (4)$$

This reparametrization of time may be inconsequential in some cases [e.g. Lagrange rotational solutions where σ is a constant since V is constant along the trajectory (see §3.6)] but may have significant effects in others [e.g. Lagrange homothety solutions where the exponential time-reparametrization regularizes triple collisions (see §3.3.2)] and could even lead to a difference between linear stability of trajectories and corresponding geodesics (see §3.6).

The curvature of the JM metric encodes information on linear stability of geodesics (see §3.5). For example, in the planar isotropic harmonic oscillator with potential $kr^2/2$ in plane polar coordinates, the gaussian curvature $R = 16Ek/(2E - kr^2)^3$ of the JM metric on configuration space is non-negative everywhere indicating stability. In the planar Kepler problem with Hamiltonian $\mathbf{p}^2/2m - k/r$, the gaussian curvature of the JM metric $ds^2 = m(E + k/r)(dr^2 + r^2d\theta^2)$ is $R = -Ek/(m(k + Er)^3)$. R is everywhere negative/positive for E positive/negative and vanishes identically for $E = 0$. This reflects the divergence of nearby hyperbolic orbits and oscillation of nearby elliptical orbits. Negativity of curvature could lead to chaos, though not always, as the hyperbolic orbits of the Kepler problem show. As noted, chaos could also arise from curvature fluctuations [14].

3 Planar three-body problem with inverse-square potential

3.1 Jacobi-Maupertuis metric on configuration space and Hopf coordinates

We consider the three-body problem with masses moving on a plane regarded as the complex plane \mathbf{C} . Its 6D configuration space (with collision points excluded) is identified with \mathbb{C}^3 . A point on \mathbb{C}^3 represents a triangle on the complex plane with the masses $m_{1,2,3}$ at its vertices $x_{1,2,3} \in \mathbf{C}$. It is convenient to work in Jacobi coordinates (Fig. 1a)

$$J_1 = x_2 - x_1, \quad J_2 = x_3 - \frac{m_1x_1 + m_2x_2}{m_1 + m_2} \quad \text{and} \quad J_3 = \frac{m_1x_1 + m_2x_2 + m_3x_3}{M_3}, \quad (5)$$

in which the kinetic energy $KE = (1/2)\sum_i m_i|\dot{x}_i|^2$ remains diagonal:

$$KE = \frac{1}{2}\sum_i M_i|\dot{J}_i|^2 \quad \text{where} \quad \frac{1}{M_1} = \frac{1}{m_1} + \frac{1}{m_2}, \quad \frac{1}{M_2} = \frac{1}{m_3} + \frac{1}{m_1 + m_2} \quad \text{and} \quad M_3 = \sum_i m_i. \quad (6)$$

The KE for motion about the center of mass (CM) is $\frac{1}{2}(M_1|\dot{J}_1|^2 + M_2|\dot{J}_2|^2)$. The moment of inertia about the origin $I = \sum_{i=1}^3 m_i|x_i|^2$ too remains diagonal in Jacobi coordinates ($I = \sum_{i=1}^3 M_i|J_i|^2$), while about the CM we have $I_{\text{CM}} = M_1|J_1|^2 + M_2|J_2|^2$. With $U = -V = \sum_{i < j} Gm_i m_j/|x_i - x_j|^2$ denoting the (negative) potential energy, the JM metric for energy E

on \mathbb{C}^3 is

$$ds^2 = (E + U) \sum_{i=1}^3 M_i |dJ_i|^2 \quad \text{where } U = \frac{Gm_1m_2}{|J_1|^2} + \frac{Gm_2m_3}{|J_2 - \mu_1 J_1|^2} + \frac{Gm_3m_1}{|J_2 + \mu_2 J_1|^2} \quad (7)$$

and $\mu_i = m_i/(m_1 + m_2)$. Due to the inverse-square potential, G *does not* have the usual dimensions. The metric is independent of the CM coordinates J_3 and \bar{J}_3 , while J_1, \bar{J}_1, J_2 and \bar{J}_2 are invariant under translations $x_i \rightarrow x_i + a$ for $a \in \mathbf{C}$. Thus translations act as isometries of (7). Similarly, we will see that scalings (for $E = 0$) and rotations also act as isometries. These isometries also act as symmetries of the Hamiltonian. For instance the dilatation $D = \sum_i \vec{x}_i \cdot \vec{p}_i = \sum_i \Re(x_i \bar{p}_i)$ generates scale transformations $x_i \rightarrow \lambda x_i$ and $p_i \rightarrow \lambda^{-1} p_i$ via Poisson brackets: $\{x_i, D\} = x_i$ and $\{p_i, D\} = -p_i$. Since $\{H, D\} = -2H$, scaling is a symmetry of the Hamiltonian only when energy vanishes.

The study of the geometry of the JM metric is greatly facilitated by first considering the geometry of its quotients by isometries (for instance, geodesics on a quotient lift to horizontal geodesics). Riemannian submersions [29] provide a framework to define and compute metrics on these quotients. Suppose (M, g) and (N, h) are two Riemannian manifolds and $f : M \rightarrow N$ a surjection. Then the linearization $df(p) : T_p M \rightarrow T_{f(p)} N$ is a surjection between tangent spaces. The vertical subspace $V(p) \subseteq T_p M$ is defined to be the kernel of df while its orthogonal complement $\ker(df)^\perp$ with respect to the metric g is the horizontal subspace $H(p)$. f is a Riemannian submersion if it preserves lengths of horizontal vectors, i.e., if the isomorphism $df(p) : \ker(df(p))^\perp \rightarrow T_{f(p)} N$ is an isometry at each point. The Riemannian submersions we are interested in are associated to quotients of a Riemannian manifold (M, g) by the action of a suitable group of isometries G . There is a natural surjection f from M to the quotient M/G . Requiring f to be a Riemannian submersion defines the quotient metric on M/G : the inner product of a pair of tangent vectors (u, v) to M/G is defined as the inner product of *any* pair of horizontal preimages under the map df .

The surjection $(J_1, \bar{J}_1, J_2, \bar{J}_2, J_3, \bar{J}_3) \mapsto (J_1, \bar{J}_1, J_2, \bar{J}_2)$ defines a submersion from configuration space \mathbb{C}^3 to its quotient \mathbb{C}^2 by translations. The vertical and horizontal subspaces are spanned by $\partial_{J_3}, \partial_{\bar{J}_3}$ and $\partial_{J_1}, \partial_{\bar{J}_1}, \partial_{J_2}, \partial_{\bar{J}_2}$ respectively. Requiring the submersion to be Riemannian, the quotient metric on \mathbb{C}^2 is

$$ds^2 = (E + U)(M_1 |dJ_1|^2 + M_2 |dJ_2|^2). \quad (8)$$

It is convenient to define rescaled coordinates on \mathbb{C}^2 , $z_i = \sqrt{M_i} J_i$, in terms of which (8) becomes $ds^2 = (E + U)(|dz_1|^2 + |dz_2|^2)$. The kinetic energy in the CM frame is $KE = (1/2)(|\dot{z}_1|^2 + |\dot{z}_2|^2)$ while $I_{\text{CM}} = |z_1|^2 + |z_2|^2$.

We now specialize to equal masses ($m_i = m$) so that $M_1 = m/2, M_2 = 2m/3$ and $\mu_i = 1/2$. The metric on \mathbb{C}^2 is seen to be conformal to the flat Euclidean metric via the conformal factor $E + U$:

$$ds^2 = \left(E + \frac{Gm^3}{2|z_1|^2} + \frac{2Gm^3}{3|z_2 - \frac{1}{\sqrt{3}}z_1|^2} + \frac{2Gm^3}{3|z_2 + \frac{1}{\sqrt{3}}z_1|^2} \right) (|dz_1|^2 + |dz_2|^2). \quad (9)$$

Rotations $U(1)$ act as a group of isometries of \mathbb{C}^2 , taking $(z_1, z_2) \mapsto (e^{i\theta} z_1, e^{i\theta} z_2)$ and leaving the conformal factor invariant. Moreover if $E = 0$, then scaling $z_i \mapsto \lambda z_i$ for $\lambda \in \mathbf{R}^+$ is also an isometry. Thus we may quotient the configuration manifold \mathbb{C}^2 successively by its isometries. We will see that $\mathbb{C}^2/U(1)$ is the shape space \mathbb{R}^3 and $\mathbb{C}^2/\text{scaling}$ is \mathbb{S}^3 . Furthermore

the quotient of \mathbb{C}^2 by both scaling and rotations leads to the shape sphere \mathbb{S}^2 (see Fig. 1c, note that collision points are excluded from $\mathbb{C}^2, \mathbb{R}^3, \mathbb{S}^3$ and \mathbb{S}^2). Points on shape space \mathbb{R}^3 represent oriented congruence classes of triangles while those on the shape sphere \mathbb{S}^2 represent oriented similarity classes of triangles. Each of these quotient spaces may be given a JM metric by requiring the projection maps to be Riemannian submersions. The geodesic dynamics on \mathbb{C}^2 is clarified by studying its projections to these quotient manifolds. We will now describe these Riemannian submersions explicitly in local coordinates. This is greatly facilitated by choosing coordinates (unlike z_1, z_2) on \mathbb{C}^2 in which the KVF's corresponding to the isometries point along coordinate vector fields. As we will see, this ensures that the vertical subspaces in the associated Riemannian submersions are spanned by coordinate vector fields. Thus we introduce the Hopf coordinates (r, η, ξ_1, ξ_2) on \mathbb{C}^2 via the transformation

$$z_1 = r e^{i(\xi_1 + \xi_2)} \sin \eta \quad \text{and} \quad z_2 = r e^{i(\xi_1 - \xi_2)} \cos \eta. \quad (10)$$

Here the radial coordinate $r = \sqrt{|z_1|^2 + |z_2|^2} = \sqrt{I_{\text{CM}}} \geq 0$ is a measure of the size of the triangle with masses at its vertices. ξ_2 determines the relative orientation of z_1 and z_2 while ξ_1 fixes the orientation of the triangle as a whole. More precisely, $2\xi_2$ is the angle from the rescaled Jacobi vector z_2 to z_1 while $2\xi_1$ is the sum of the angles subtended by z_1 and z_2 with the horizontal axis in Fig 1a. Thus we may take $0 \leq \xi_1 + \xi_2 \leq 2\pi$ and $0 \leq \xi_1 - \xi_2 \leq 2\pi$ or equivalently, $-\pi \leq \xi_2 \leq \pi$ and $|\xi_2| \leq \xi_1 \leq 2\pi - |\xi_2|$. Finally, $0 \leq \eta \leq \pi/2$ measures the relative magnitudes of z_1 and z_2 , indeed $\tan \eta = |z_1|/|z_2|$. When r is held fixed, η, ξ_1 and ξ_2 furnish the standard Hopf coordinates parametrizing the three sphere $|z_1|^2 + |z_2|^2 = r^2$. For fixed r and η , $\xi_1 + \xi_2$ and $\xi_1 - \xi_2$ are periodic coordinates on tori. These tori foliate the above three-sphere as η ranges between 0 and $\pi/2$. Furthermore, as shown in §3.2, 2η and $2\xi_2$ are polar and azimuthal angles on the two-sphere obtained as the quotient of \mathbb{S}^3 by rotations via the Hopf map.

Let us briefly motivate these coordinates and the identification of the above quotient spaces. We begin by noting that the JM metric (9) on \mathbb{C}^2 is conformal to the flat Euclidean metric $|dz_1|^2 + |dz_2|^2$. Recall that the cone on a Riemannian manifold (M, ds_M^2) is the Cartesian product $\mathbf{R}^+ \times M$ with metric $dr^2 + r^2 ds_M^2$ where $r > 0$ parameterizes \mathbf{R}^+ . In particular, Euclidean \mathbf{C}^2 may be viewed as a cone on the round three sphere \mathbf{S}^3 . If \mathbf{S}^3 is parameterized by Hopf coordinates η, ξ_1 and ξ_2 , then this cone structure allows us to use r, η, ξ_1 and ξ_2 as coordinates on \mathbf{C}^2 . Moreover, the Hopf map defines a Riemannian submersion from the round \mathbf{S}^3 to the round two sphere \mathbf{S}^2 ¹. Indeed, if we use Hopf coordinates η, ξ_1, ξ_2 on \mathbf{S}^3 , then the Hopf map takes $(\eta, \xi_1, \xi_2) \mapsto (\eta, \xi_2) \in \mathbf{S}^2$. In general, if $M \rightarrow N$ is a Riemannian submersion, then there is a natural submersion from the cone on M to the cone on N ². In particular, the

¹ The Hopf map $\mathbf{S}^3 \rightarrow \mathbf{S}^2$ is often expressed in Cartesian coordinates. If $|z_1|^2 + |z_2|^2 = 1$ defines the unit- $\mathbf{S}^3 \subset \mathbf{C}^2$ and $w_1^2 + w_2^2 + w_3^2 = 1/4$ defines a 2-sphere of radius 1/2 in \mathbf{R}^3 , then $w_3 = (|z_2|^2 - |z_1|^2)/2$ and $w_1 + iw_2 = z_1 \bar{z}_2$. Using Eq.10, we may express the Cartesian coordinates w_i in terms of Hopf coordinates:

$$2w_3 = r^2 \cos 2\eta, \quad 2w_1 = r^2 \sin(2\eta) \cos(2\xi_2) \quad \text{and} \quad 2w_2 = r^2 \sin(2\eta) \sin(2\xi_2).$$

²Let $f : (M, g) \mapsto (N, h)$ be a Riemannian submersion with local coordinates m^i and n^j . Let (r, m^i) and (r, n^j) be local coordinates on the cones $C(M)$ and $C(N)$. Then $\tilde{f} : (r, m) \mapsto (r, n)$ defines a submersion from $C(M)$ to $C(N)$. Consider a horizontal vector $a\partial_r + b_i\partial_{m_i}$ in $T_{(r,m)}C(M)$. We will show that $d\tilde{f}$ preserves its length. Now, if $df(b_i\partial_{m_i}) = c_i\partial_{n_i}$ then $d\tilde{f}(a\partial_r + b_i\partial_{m_i}) = a\partial_r + c_i\partial_{n_i}$. Since $\partial_r \perp \partial_{m_i}$, $\|a\partial_r + b_i\partial_{m_i}\|^2 = a^2 + r^2\|b_i\partial_{m_i}\|^2 = a^2 + r^2\|c_i\partial_{n_i}\|^2$ as f is a Riemannian submersion. Moreover $a^2 + r^2\|c_i\partial_{n_i}\|^2 = \|a\partial_r + c_i\partial_{n_i}\|^2$ since $\partial_r \perp \partial_{n_i}$. Thus \tilde{f} is a Riemannian submersion.

Hopf map extends to a Riemannian submersion from the cone on the round \mathbf{S}^3 to the cone on the round \mathbf{S}^2 , i.e. from Euclidean \mathbf{C}^2 to Euclidean \mathbf{R}^3 taking $(r, \eta, \xi_1, \xi_2) \mapsto (r, \eta, \xi_2)$. As the conformal factor is independent of rotations, the same map defines a Riemannian submersion from \mathbb{C}^2 with the JM metric to shape space \mathbb{R}^3 with its quotient JM metric. Finally, for $E = 0$, scaling $\vec{r} \rightarrow \lambda \vec{r}$ defines an isometry of the quotient JM metric on shape space \mathbb{R}^3 . Quotienting by this isometry we arrive at the shape sphere \mathbb{S}^2 with Montgomery's 'pair of pants' metric. Alternatively, we may quotient \mathbb{C}^2 first by the scaling isometry of its JM metric to get \mathbb{S}^3 and then by rotations to get \mathbb{S}^2 (see Fig. 1c).

With these motivations, we express the equal-mass JM metric on \mathbb{C}^2 in Hopf coordinates [generalization to unequal masses is obtained by replacing Gm^3h below with $\tilde{h}(\eta, \xi_2)$ given in Eq. (31)]:

$$ds^2 = \left(E + \frac{Gm^3h(\eta, \xi_2)}{r^2} \right) (dr^2 + r^2 (d\eta^2 + d\xi_1^2 - 2 \cos 2\eta \, d\xi_1 \, d\xi_2 + d\xi_2^2)). \quad (11)$$

It is convenient to write $h(\eta, \xi_2) = v_1 + v_2 + v_3$ where $v_1 = r^2/(m|x_2 - x_3|^2)$ is proportional to the pairwise potential between m_2 and m_3 and cyclic permutations thereof. The v_i are rotation and scale-invariant, and therefore functions only of η and ξ_2 in Hopf coordinates:

$$v_{1,2} = \frac{2}{(2 + \cos 2\eta \mp \sqrt{3} \sin 2\eta \cos 2\xi_2)} \quad \text{and} \quad v_3 = \frac{1}{2 \sin^2 \eta}. \quad (12)$$

Notice that $h \rightarrow \infty$ at pairwise collisions. The v_i 's have the common range $1/2 \leq v_i < \infty$ with $v_3 = 1/2$ when m_3 is at the CM of m_1 and m_2 etc. We also have $h \geq 3$ with equality when $v_1 = v_2 = v_3$, corresponding to Lagrange configurations with masses at vertices of an equilateral triangle. To see this, we compute the moment of inertia I_{CM} in two ways. On the one hand $I_{\text{CM}} = |z_1|^2 + |z_2|^2 = r^2$. On the other hand, for equal masses the CM lies at the centroid of the triangle defined by masses. Thus I_{CM} is $(4m/9) \times$ the sum of the squares of the medians, which by Apollonius' theorem is equal to $(3/4) \times$ the sum of the squares of the sides. Hence $I_{\text{CM}} = \sum_{i=1}^3 r^2/3v_i$. Comparing, we get $\sum_{i=1}^3 1/v_i = 3$. Since the arithmetic mean is bounded below by the harmonic mean,

$$h/3 = (v_1 + v_2 + v_3)/3 \geq 3(v_1^{-1} + v_2^{-1} + v_3^{-1})^{-1} = 1. \quad (13)$$

Lagrange, Euler, collinear and collision configurations: The geometry of the JM metric displays interesting behavior at Lagrange and collision configurations on \mathbb{C}^2 and its quotients. We identify their locations in Hopf coordinates for *equal* masses. The Jacobi vectors in Hopf coordinates are

$$J_1 = \sqrt{\frac{2}{m}} r e^{i(\xi_1 + \xi_2)} \sin \eta \quad \text{and} \quad J_2 = \sqrt{\frac{3}{2m}} r e^{i(\xi_1 - \xi_2)} \cos \eta. \quad (14)$$

At a Lagrange configuration, $m_{1,2,3}$ are at vertices of an equilateral triangle. So $|J_2| = \sqrt{3}|J_1|/2$ (i.e. $\eta = \pi/4$) and J_2 is \perp to J_1 (i.e. $\xi_2 = \pm\pi/4$, the sign being fixed by the orientation of the triangle). So Lagrange configurations $L_{4,5}$ on \mathbb{C}^2 occur when $\eta = \pi/4$ and $\xi_2 = \pm\pi/4$ with r and ξ_1 arbitrary. On quotients of \mathbb{C}^2 , $L_{4,5}$ occur at the images under the corresponding projections. Since 2η and $2\xi_2$ are polar and azimuthal angles on the shape sphere, $L_{4,5}$ are at diametrically opposite equatorial locations (see Fig. 1b). Collinear configurations (syzygies)

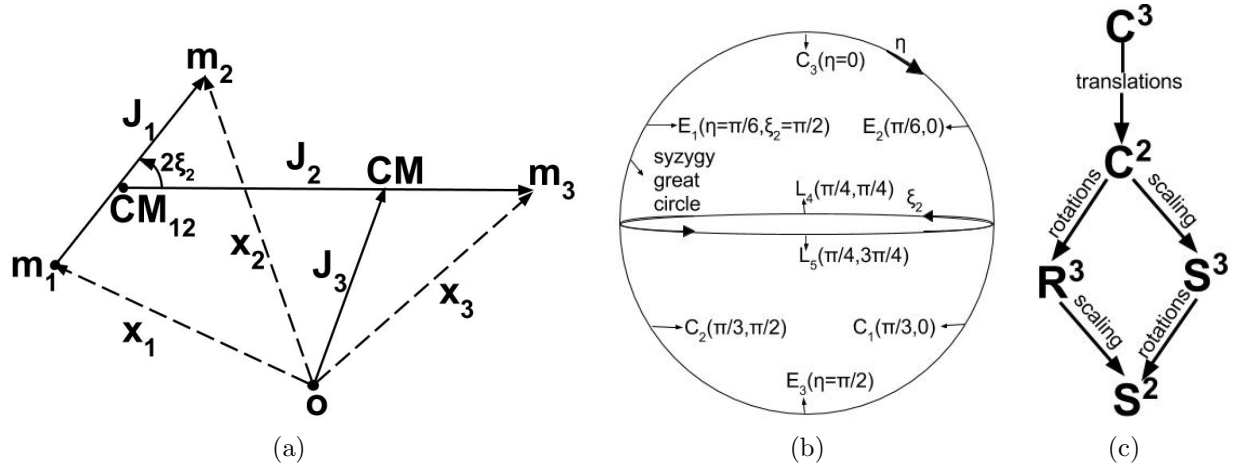


Figure 1: (a) Position vectors $x_{1,2,3}$ of masses relative to origin and Jacobi vectors $J_{1,2,3}$. (b) The shape sphere is topologically a 2-sphere with the three collision points $C_{1,2,3}$ removed, endowed with the quotient JM metric of *negative* gaussian curvature. Coordinates and physical locations on the shape sphere are illustrated. 2η is the polar angle ($0 \leq \eta \leq \pi/2$). $2\xi_2$ is the azimuthal angle ($0 \leq \xi_2 \leq \pi$). The ‘great circle’ composed of the two longitudes $\xi_2 = 0$ and $\xi_2 = \pi/2$ consists of collinear configurations (syzygies) which include $C_{1,2,3}$ and the Euler points $E_{1,2,3}$. Lagrange points $L_{4,5}$ lie on the equator $\eta = \pi/4$. The shape space \mathbb{R}^3 is a cone on the shape sphere. The origin $r = 0$ of shape space is the triple collision point. (c) Flowchart of submersions.

occur when J_1 and J_2 are (anti)parallel, i.e. when $\xi_2 = 0$ or $\pi/2$, with other coordinates arbitrary. On the shape sphere, syzygies occur on the ‘great circle’ through the poles corresponding to the longitudes $2\xi_2 = 0$ and π . Collisions are special collinear configurations. By C_i we denote a collision of particles other than the i^{th} one. So C_3 corresponds to $J_1 = 0$ which lies at the ‘north pole’ ($\eta = 0$) on \mathbb{S}^2 . m_2 and m_3 collide when $J_2 = J_1/2$ so $\eta = \pi/3$ and $\xi_2 = 0$ at C_1 . Similarly, at C_2 , $J_2 = -J_1/2$ which corresponds to $\eta = \pi/3$ and $\xi_2 = \pi/2$. The Euler configurations E_i for equal masses are collinear configurations where mass m_i is at the midpoint of the other two.

Finally, we note that the azimuth and co-latitude (θ and ϕ) [20] are often used as coordinates on the shape sphere, so that $L_{4,5}$ are at the poles while $C_{1,2,3}$ and $E_{1,2,3}$ lie on the equator. This coordinate system makes the symmetry under permutations of masses explicit, but is not convenient near any of the collisions (e.g. sectional curvatures can be discontinuous). On the other hand, our coordinates η and ξ_2 , which are related to θ and ϕ by suitable rotations,

$$\sin \phi = \cos(2\eta - \pi/2) \sin(2\xi_2), \quad \cos \phi \sin \theta = \cos(2\eta - \pi/2) \cos(2\xi_2), \quad \cos \phi \cos \theta = \sin(2\eta - \frac{\pi}{2}),$$

are convenient near C_3 but not near E_3 or $C_{1,2}$ (sectional curvatures can be discontinuous, see §3.5). The neighborhoods of the latter configurations may be studied by re-ordering the masses.

3.2 Quotient JM metrics on shape space, the three-sphere and the shape sphere

Submersion from \mathbb{C}^2 to shape space \mathbb{R}^3 : Rotations $z_j \rightarrow e^{i\theta} z_j$ act as isometries of the JM metric (11) on \mathbb{C}^2 . In the Hopf coordinates of Eq. (10),

$$z_1 = r e^{i(\xi_1 + \xi_2)} \sin \eta \quad \text{and} \quad z_2 = r e^{i(\xi_1 - \xi_2)} \cos \eta, \quad (15)$$

rotations are generated by translations $\xi_1 \rightarrow \xi_1 + \theta$ and a discrete shift $\xi_2 \rightarrow \xi_2 + \pi \pmod{2\pi}$. The shift in ξ_2 rotates $z_i \mapsto -z_i$, which is not achievable by a translation in ξ_1 due to its restricted range, $|\xi_2| \leq \xi_1 \leq 2\pi - |\xi_2|$ and $-\pi \leq \xi_2 \leq \pi$. To quotient by this isometry, we define a submersion from $\mathbb{C}^2 \rightarrow \mathbb{R}^3$ taking

$$(r, \eta, \xi_1, \xi_2) \mapsto (r, \eta, \xi_2) \quad \text{if } \xi_2 \geq 0 \quad \text{and} \quad (r, \eta, \xi_1, \xi_2) \mapsto (r, \eta, \xi_2 + \pi) \quad \text{if } \xi_2 < 0. \quad (16)$$

The radial, polar and azimuthal coordinates on \mathbb{R}^3 are given by r , 2η and $2\xi_2$ with m_1 - m_2 collisions occurring on the ray $\eta = 0$. Under the linearization of this submersion at a point $p \in \mathbb{C}^2$, $V(p)$ is spanned by ∂_{ξ_1} and $H(p)$ by ∂_r , ∂_η and $\cos 2\eta \partial_{\xi_1} + \partial_{\xi_2}$. These horizontal basis vectors are mapped respectively to ∂_r , ∂_η and ∂_{ξ_2} under the linearization of the map. Requiring lengths of horizontal vectors to be preserved we arrive at the following quotient JM metric on \mathbb{R}^3 , conformal to the flat metric on \mathbb{R}^3 :

$$ds^2 = \left(E + \frac{Gm^3 h(\eta, \xi_2)}{r^2} \right) (dr^2 + r^2 (d\eta^2 + \sin^2 2\eta d\xi_2^2)). \quad (17)$$

This metric may also be viewed as conformal to a cone on a round 2-sphere of radius one-half, since $0 \leq 2\eta \leq \pi$ and $0 \leq 2\xi_2 \leq 2\pi$ are the polar and azimuthal angles.

Submersion from shape space to the shape sphere: The group \mathbf{R}^+ of scalings $(r, \eta, \xi_2) \mapsto (\lambda r, \eta, \xi_2)$ acts as an isometry of the *zero-energy* JM metric (17) on shape space \mathbb{R}^3 . The orbits are radial rays emanating from the origin (and the triple collision point at the origin, which we exclude). The quotient space $\mathbb{R}^3/\text{scaling}$ is the shape sphere \mathbb{S}^2 . We define a submersion from shape space to the shape sphere taking $(r, \eta, \xi_2) \mapsto (\eta, \xi_2)$. Under the linearization of this map at $p \in \mathbb{R}^3$, $V(p) = \text{span}(\partial_r)$. Its orthogonal complement $H(p)$ is spanned by ∂_η and ∂_{ξ_2} which project to ∂_η and ∂_{ξ_2} on \mathbb{S}^2 . Requiring the submersion to be Riemannian, we get the quotient ‘pair of pants’ JM metric on the shape sphere which is conformal to the round metric on a 2-sphere of radius one-half:

$$ds^2 = Gm^3 h(\eta, \xi_2) (d\eta^2 + \sin^2 2\eta d\xi_2^2). \quad (18)$$

Submersion from \mathbb{C}^2 to \mathbb{S}^3 and then to \mathbb{S}^2 : For zero energy, it is also possible to quotient the JM metric (11) on \mathbb{C}^2 , first by its scaling isometries to get \mathbb{S}^3 and then by rotations to arrive at the shape sphere. Interestingly, it follows from the Lagrange-Jacobi identity that when E and \dot{I} vanish, r is constant and the motion is confined to a 3-sphere embedded in \mathbb{C}^2 . To quotient by the scaling isometries $(r, \eta, \xi_1, \xi_2) \mapsto (\lambda r, \eta, \xi_1, \xi_2)$ of \mathbb{C}^2 , we define the submersion $(r, \eta, \xi_1, \xi_2) \mapsto (\eta, \xi_1, \xi_2)$ to \mathbb{S}^3 , with ranges of coordinates as on \mathbb{C}^2 . The vertical subspace is spanned by ∂_r while ∂_η , ∂_{ξ_1} and ∂_{ξ_2} span the horizontal subspace. The latter are mapped to ∂_η , ∂_{ξ_1} and ∂_{ξ_2} on \mathbb{S}^3 . The submersion is Riemannian provided we endow \mathbb{S}^3 with the following conformally-round metric

$$ds^2 = Gm^3 h(\eta, \xi_2) (d\eta^2 + d\xi_1^2 - 2 \cos 2\eta d\xi_1 d\xi_2 + d\xi_2^2). \quad (19)$$

Rotations generated by $\xi_1 \rightarrow \xi_1 + \theta$ and $\xi_2 \rightarrow \xi_2 + \pi \pmod{2\pi}$ act as isometries of this metric on \mathbb{S}^3 . We quotient by rotations to get the metric (18) on \mathbb{S}^2 via the Riemannian submersion defined by

$$(\eta, \xi_1, \xi_2) \mapsto (\eta, \xi_2) \quad \text{if } \xi_2 \geq 0 \quad \text{and} \quad (\eta, \xi_1, \xi_2) \mapsto (\eta, \xi_2 + \pi) \quad \text{if } \xi_2 < 0. \quad (20)$$

3.3 JM metric in the near-collision limit and its completeness

The equal-mass JM metric components on configuration space \mathbb{C}^2 and its quotients blow up at 2- and 3-body collisions. However, we study the geometry in the neighbourhood of collision configurations and show that the curvature remains finite in the limit. Remarkably, it takes infinite geodesic time for collisions to occur which we show by establishing the geodesic completeness of the JM metric on \mathbb{C}^2 and its quotients. By contrast, collisions can occur in finite time for the Newtonian 3-body evolution. The JM geodesic flow avoids finite time collisions by reparametrizing time along Newtonian trajectories (see Eq. 3). Thus the geodesic reformulation of the inverse-square 3-body problem ‘regularizes’ pairwise and triple collisions.

3.3.1 Geometry near pairwise collisions

For equal masses (see §3.1), the first pair of masses collide when $\eta = 0$ (with other coordinates arbitrary) while the other two binary collisions occur at C_1 and C_2 (see Fig. 1b). Triple collisions occur when $r = 0$. Unlike for the Newtonian potential, sectional curvatures on coordinate 2-planes are finite at pairwise and triple collisions, though some JM metric (11) and Riemann tensor components blow up. It is therefore interesting to study the near-collision geometry of the JM metric.

The geometry of the equal-mass JM metric in the neighbourhood of a binary collision is the same irrespective of which pair of bodies collide. Since Hopf coordinates are particularly convenient around $\eta = 0$, we focus on collisions between the first pair of masses. Montgomery (see eqn. 3.10c of [20]) studied the near-collision geometry on \mathbb{S}^2 and showed that it is geodesically complete. Let us briefly recall the argument. Expanding the equal-mass \mathbb{S}^2 metric (18) around the collision point $\eta = 0$, we get

$$ds^2 \approx \left(\frac{Gm^3}{2\eta^2} \right) (d\eta^2 + 4\eta^2 d\xi_2^2) = \frac{Gm^3}{2\rho^2} (d\rho^2 + \rho^2 d\chi^2) \quad (21)$$

where $\rho = 2\eta$ and $\chi = 2\xi_2$. ∂_χ is a KVF, so ‘radial’ curves with constant χ are geodesics. Approaching $\rho = 0$ along a ‘radial’ geodesic shows that the collision point $\rho = 0$ is at an infinite distance ($\sqrt{Gm^3/2} \int_{\rho_0}^0 d\rho/\rho$) from any point (ρ_0, χ) in its neighborhood ($0 < \rho_0 \ll 1$). The symmetry of the metric under exchange of masses ensures that the same holds for the other two collision points: geodesics may be extended indefinitely. Thus the shape sphere (\mathbb{S}^2 with three collision points excluded) is geodesically complete. To clarify the near-collision geometry let $d\lambda = -d\rho/\sqrt{2}\rho$ or $\lambda = -\log(\rho/\rho_0)/\sqrt{2}$. This effectively stretches out the neighborhood of the collision point $\lambda = \infty$. The asymptotic metric $ds^2 = Gm^3 (d\lambda^2 + d\chi^2/2)$ for $0 \leq \chi \leq 2\pi$ and $\lambda \geq 0$ is the metric on a semi-infinite right-circular cylinder of radius $\sqrt{Gm^3/2}$ with λ the coordinate along the height and χ the azimuthal angle. Thus the JM metric looks like that of a semi-infinite cylinder near any of the collision points.

More generally, for *unequal* masses, the near-collision metric (21) is $ds^2 \approx \frac{Gm_1 m_2 M_1}{2\eta^2} (d\eta^2 + 4\eta^2 d\xi_2^2)$ (see Eq. (7-10)) and essentially the same argument implies that the JM metric on the shape sphere is geodesically complete for arbitrary masses.

Since \mathbb{S}^2 arises as a Riemannian submersion of \mathbb{R}^3 , \mathbb{S}^3 and \mathbb{C}^2 , the infinite distance to binary collision points on the shape sphere can be used to show that the same holds on each of the higher dimensional manifolds. To see this, consider the submersion from (say) \mathbb{C}^2 to \mathbb{S}^2 . Any

curve $\tilde{\gamma}$ on \mathbb{C}^2 maps to a curve γ on \mathbb{S}^2 with $l(\tilde{\gamma}) \geq l(\gamma)$ since the lengths of horizontal vectors are preserved. If there was a binary collision point at finite distance on \mathbb{C}^2 , there would have to be a geodesic of finite length ending at it. However, such a geodesic would project to a curve on the shape sphere of finite length ending at a collision point, contradicting its completeness.

Thus we have shown that the JM metrics (necessarily of zero energy) on \mathbb{S}^2 and \mathbb{S}^3 with binary collision points removed, are geodesically complete for arbitrary masses. On the other hand, to examine completeness on \mathbb{C}^2 and \mathbb{R}^3 we must allow for triple collisions as well as non-zero energy. Geodesic completeness in these cases is shown in §3.3.2. In the sequel we examine the near-collision geometry on \mathbb{R}^3 , \mathbb{S}^3 and \mathbb{C}^2 in somewhat greater detail by Laurent expanding the JM metric components around $\eta = 0$ and keeping only leading terms.

Shape space geometry near binary collisions: The equal-mass shape space metric around $\eta = 0$, in the leading order, becomes

$$ds^2 \approx \frac{Gm^3}{2\eta^2 r^2} (dr^2 + r^2 (d\eta^2 + 4\eta^2 d\xi_2^2)) = Gm^3 \left(\frac{2dr^2}{\rho^2 r^2} + \frac{d\rho^2}{2\rho^2} + \frac{d\chi^2}{2} \right), \quad (22)$$

where $\rho = 2\eta$ and $\chi = 2\xi_2$. We define new coordinates λ and κ by $d\lambda = -d\rho/\sqrt{2}\rho$, $d\kappa = dr/r$ so that $\rho = \rho_0 e^{-\sqrt{2}\lambda}$. In these coordinates the collision occurs at $\lambda = \infty$. The asymptotic metric is

$$ds^2 \approx Gm^3 \left(\frac{2}{\rho_0^2} e^{2\sqrt{2}\lambda} d\kappa^2 + d\lambda^2 + \frac{1}{2} d\chi^2 \right) \quad (23)$$

where $0 \leq \chi \leq 2\pi$ (periodic), $\lambda \geq 0$ and $-\infty < \kappa < \infty$. This metric has a constant scalar curvature of $-4/Gm^3$. The sectional curvature in the $\partial_\lambda - \partial_\kappa$ plane is equal to $-2/Gm^3$, it vanishes in the other two coordinate planes. These values of scalar and sectional curvatures agree with the limiting values at the 1-2 collision point calculated for the full metric on shape space. The near-collision topology of shape space is that of the product manifold $\mathbf{S}_\chi^1 \times \mathbf{R}_\lambda^+ \times \mathbf{R}_\kappa$.

Near-collision geometry on \mathbb{C}^2 : The equal-mass JM metric in leading order around $\eta = 0$ is

$$ds^2 \approx \frac{Gm^3}{2\eta^2 r^2} (dr^2 + r^2 (d\eta^2 + d\xi_1^2 - 2(1 - 2\eta^2)d\xi_1 d\xi_2 + d\xi_2^2)). \quad (24)$$

Let us define new coordinates λ, κ, ξ_\pm such that $d\lambda = -d\eta/\sqrt{2}\eta$, $d\kappa = -dr/r$ and $\xi_\pm = \xi_1 \pm \xi_2$. $0 \leq \xi_\pm \leq 2\pi$ are periodic coordinates parametrizing a torus. The asymptotic metric is

$$ds^2 \approx Gm^3 \left(\frac{d\kappa^2}{2\eta^2} + d\lambda^2 + \frac{1}{2\eta^2} d\xi_-^2 + \frac{1}{2} d\xi_+^2 \right) \quad (25)$$

where $\eta = \eta_0 e^{-\sqrt{2}\lambda}$. This metric has a constant scalar curvature $-12/Gm^3$. The sectional curvature of any coordinate plane containing ∂_{ξ_+} vanishes due to the product form of the metric. The sectional curvatures of the remaining coordinate planes ($\partial_\kappa - \partial_\lambda$, $\partial_\kappa - \partial_{\xi_-}$, $\partial_{\xi_-} - \partial_\lambda$) are equal to $-2/Gm^3$. The scalar and sectional curvatures (of corresponding planes) of this metric agree with the limiting values computed from the full metric on \mathbb{C}^2 .

Near-collision geometry on \mathbb{S}^3 : The submersion $\mathbb{C}^2 \rightarrow \mathbb{S}^3$ takes $(\kappa, \lambda, \xi_\pm) \mapsto (\lambda, \xi_\pm)$. As the coordinate vector fields on \mathbb{C}^2 are orthogonal, from (25) the asymptotic metric on \mathbb{S}^3 near the 1-2 collision point is

$$ds^2 \approx Gm^3 \left(d\lambda^2 + \frac{1}{2\eta^2} d\xi_-^2 + \frac{1}{2} d\xi_+^2 \right). \quad (26)$$

This metric has a constant scalar curvature equal to $-4/Gm^3$. The sectional curvatures on the $\lambda - \xi_-$ coordinate 2-plane is $-2/Gm^3$ while it vanishes on the other two coordinate 2-planes.

3.3.2 Geometry on \mathbb{R}^3 and \mathbb{C}^2 near triple collisions

We argue that the triple collision configuration (which occurs at $r = 0$ on \mathbb{C}^2 or shape space \mathbb{R}^3) is at infinite distance from other configurations with respect to the equal-mass JM metrics (Eqs. (11),(17)), which may be written in the form:

$$ds^2 = (Gm^3 h / r^2) dr^2 + Gm^3 h g_{ij} dx^i dx^j. \quad (27)$$

g_{ij} is the positive (round) metric on \mathbf{S}^3 ($x^i = (\eta, \xi_1, \xi_2)$) or \mathbf{S}^2 ($x^i = (\eta, \xi_2)$) of radius one-half:

$$g_{ij}^{\mathbb{C}^2} = \begin{pmatrix} 1 & 0 & 0 \\ 0 & 1 & -\cos 2\eta \\ 0 & -\cos 2\eta & 1 \end{pmatrix} \quad \text{and} \quad g_{ij}^{\mathbb{R}^3} = \begin{pmatrix} 1 & 0 \\ 0 & \sin 2\eta \end{pmatrix}. \quad (28)$$

Together with our results on pairwise collisions (§3.3.1), it will follow that the manifolds are geodesically complete. As a consequence, the geodesic flow reformulation of the 3-body problem regularizes triple collisions. To show that triple collision points are at infinite distance we will use the previously obtained lower bound on the conformal factor, $h(\xi_2, \eta) \geq 3$ (see Eqn. 13).

Let $\gamma(t)$ be a curve joining a non-collision point $\gamma(t_0) \equiv (r_0, x_0^i)$ and the triple collision point $\gamma(t_1) \equiv (r = 0, x_1^i)$. We show that its length $l(\gamma)$ is infinite. Since $Gm^3 h g_{ij}$ is a positive matrix,

$$l(\gamma) = \int_{t_0}^{t_1} dt \sqrt{\frac{Gm^3 h}{r^2} \dot{r}^2 + Gm^3 h g_{ij} \dot{x}^i \dot{x}^j} \geq \int_{t_0}^{t_1} dt \sqrt{\frac{Gm^3 h}{r^2} \dot{r}^2}. \quad (29)$$

Now using $|\dot{r}| \geq -\dot{r}$ and $h \geq 3$, we get

$$l(\gamma) \geq -\sqrt{3Gm^3} \int_{t_0}^{t_1} \frac{\dot{r}}{r} dt = \sqrt{3Gm^3} \int_0^{r_0} \frac{dr}{r} = \infty. \quad (30)$$

In particular, a geodesic from a non-collision point to the triple collision point has infinite length. Despite appearances, the above inequality $l(\gamma) \geq \sqrt{3Gm^3} \int_0^{r_0} dr/r$ does not imply that radial curves are always geodesics. This is essentially because h along γ may be less than that on the corresponding radial curve. However, if (η, ξ_1, ξ_2) is an angular location where h is minimal (locally), then the radial curve with those angular coordinates is indeed a geodesic because a small perturbation to the radial curve increases h and consequently its length. The global minima of h ($h = 3$) occur at the Lagrange configurations $L_{4,5}$ and local minima ($h = 9/2$) are at the Euler configurations $E_{1,2,3}$ indicating that radial curves at these angular locations are geodesics. In fact, the Christoffel symbols Γ_{rr}^i vanish for $i = \eta, \xi_1, \xi_2$ at $L_{4,5}$ and at $E_{1,2,3}$ so that radial curves $\gamma = (r(t), x_0^i)$ satisfying $\ddot{r} + \Gamma_{rr}^r \dot{r}^2 = 0$ are geodesics.

These radial geodesics at minima of h describe Lagrange and Euler homotheties (where the masses move radially inwards/outwards to/from their CM which is the center of similitude). These homotheties take infinite (geodesic) time to reach the triple collision. By contrast, the corresponding Lagrange and Euler homothety solutions to Newton's equations reach the collision point in finite time. This difference is due to an exponential time-reparametrization of geodesics relative to trajectories. In fact, if t is trajectory time and s arc-length along

geodesics, then from §2 and §3.1, $\sigma = ds/dt = \sqrt{2}(E + 3Gm^3/r^2)$ since $h = 3$. Near a triple collision (small r), $ds^2 \approx 3Gm^3 dr^2/r^2$ so that $s \approx -\frac{1}{2}\sqrt{3Gm^3} \log(1 - t/t_c) \rightarrow \infty$ as $t \rightarrow t_c = r(0)^2/2\sqrt{6Gm^3}$ which is the approximate time to collision. In fact, the exact collision time $t_c = \sqrt{6Gm^3} \left(-1 + \sqrt{1 + \kappa r(0)^2/6Gm^3} \right) / \kappa$ may be obtained by reducing Newton's equations for Lagrange homotheties to the one body problem $r^3\ddot{r} = -6Gm^3$ whose conserved energy is $\kappa = \dot{r}^2 - 6Gm^3/r^2$. These homothety solutions illustrate how the geodesic flow reformulation regularizes the original Newtonian 3 body dynamics in the inverse-square potential.

More generally, for unequal masses (7)-(10) give the JM metric $ds^2 = \tilde{h}dr^2/r^2 + \tilde{g}_{ij}dx^i dx^j$ where

$$\tilde{h} = \frac{Gm_1m_2M_1}{\sin^2\eta} + \frac{Gm_2m_3M_2}{\left| \cos\eta - \mu_1\sqrt{M_2/M_1}e^{2i\xi_2}\sin\eta \right|^2} + \frac{Gm_1m_3M_2}{\left| \cos\eta + \mu_2\sqrt{M_2/M_1}e^{2i\xi_2}\sin\eta \right|^2}. \quad (31)$$

Irrespective of the masses, \tilde{g}_{ij} (28) is positive and \tilde{h} has a strictly positive lower bound (e.g. $Gm_1m_2M_1$). Thus by the same argument as above, triple collisions are at infinite distance. Combining this with the corresponding results for pairwise collision points (§3.3.1), we conclude that the zero-energy JM metrics on \mathbb{C}^2 and \mathbb{R}^3 are geodesically complete for arbitrary masses.

For non-zero energy, $ds^2 = (E + \tilde{h}/r^2)(dr^2 + r^2\tilde{g}_{ij}dx^i dx^j)$ which can be approximated with the zero-energy JM metrics both near binary (say, $\eta = 0$) and triple ($r = 0$) collisions. If γ is a curve ending at the triple collision, $l(\gamma) \geq l(\tilde{\gamma})$ where $\tilde{\gamma}$ is a 'tail end' of γ lying in a sufficiently small neighborhood of $r = 0$ (i.e., $r \ll |\tilde{h}/E|^{1/2}$ which is guaranteed, say, if $r \ll |Gm_1m_2M_1/E|^{1/2}$). But then, $l(\tilde{\gamma})$ may be estimated using the zero-energy JM metric giving $l(\tilde{\gamma}) = \infty$. Thus $l(\gamma) = \infty$. A similar argument shows that curves ending at binary collisions have infinite length. Thus we conclude that the JM metrics on \mathbb{C}^2 and \mathbb{R}^3 are geodesically complete for arbitrary energies and masses.

3.4 Scalar curvature for equal masses and zero energy

A geodesic through P in the direction u perturbed along v is linearly stable/unstable [see §3.6] according as the sectional curvature $K_P(u, v)$ is positive/negative. The scalar curvature R at P is proportional to an average of sectional curvatures in planes through P (§3.5). Thus R encodes an average notion of geodesic stability. Here, we evaluate the scalar curvature R of the equal-mass zero-energy JM metric on \mathbb{C}^2 and its submersions to \mathbb{R}^3 , \mathbb{S}^3 and \mathbb{S}^2 . In each case, due to the rotation and scaling isometries, R is a function only of the coordinates η and ξ_2 that parametrize the shape sphere. In [20] Montgomery proves that $R_{\mathbb{S}^2} \leq 0$ with equality at Lagrange and collision points (see Fig. 2). We generalize this result and prove that the scalar curvatures on \mathbb{C}^2 , \mathbb{R}^3 and \mathbb{S}^3 are strictly negative and bounded below (see Fig. 3) indicating widespread linear instability of the geodesic dynamics. (Note that hyperbolicity of the configuration space quotiented by translations, rotations and scaling does not extend in a simple manner to the 4-body problem [30].)

Scalar curvature on \mathbb{S}^2 : The quotient JM metric on \mathbb{S}^2 (18) is conformal to the round (kinetic) metric on a sphere of radius $1/2$:

$$ds_{\mathbb{S}^2}^2 = Gm^3 h(\eta, \xi_2) ds_{\text{kin}}^2 \quad \text{where} \quad ds_{\text{kin}}^2 = d\eta^2 + \sin^2 2\eta d\xi_2^2. \quad (32)$$

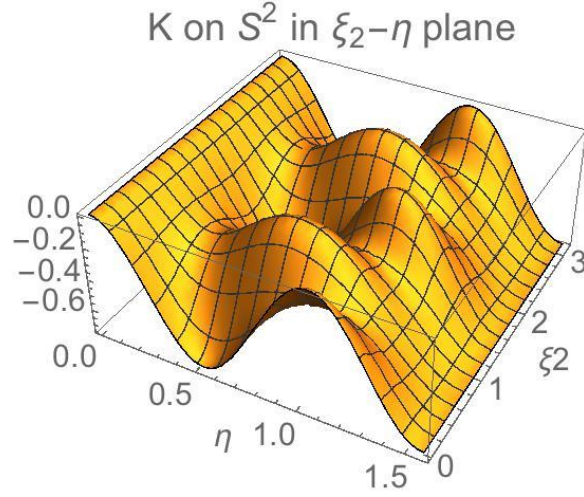


Figure 2: Gaussian curvature K (in units of $1/Gm^3$) on \mathbb{S}^2 for equal masses and $E = 0$. $K = 0$ at $L_{4,5}$ and $C_{1,2,3}$.

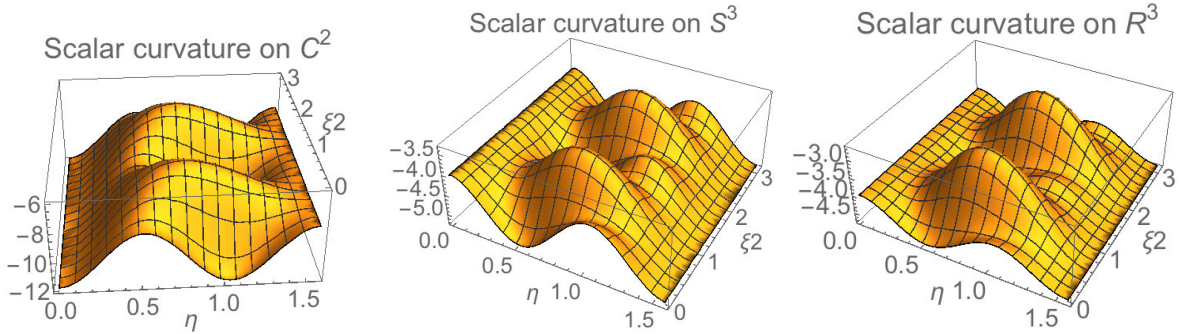


Figure 3: Scalar curvatures R on \mathbb{C}^2 , \mathbb{S}^3 and \mathbb{R}^3 in units of $1/Gm^3$. R is strictly negative and has a global maximum at $L_{4,5}$ in all cases. It attains a global minimum at $C_{1,2,3}$ on \mathbb{C}^2 and a local maximum at collisions on \mathbb{R}^3 and \mathbb{S}^3 . $E_{1,2,3}$ are saddles on \mathbb{C}^2 and global minima on \mathbb{R}^3 and \mathbb{S}^3 .

Here the conformal factor ($h = -(r^2/Gm^3) \times$ potential energy) (12) is a strictly positive function on the shape sphere with double poles at collision points. The scalar curvature of (32) is

$$R_{\mathbb{S}^2} = \frac{1}{Gm^3 h^3} (8h^2 + |\nabla h|^2 - h\Delta h), \quad (33)$$

where Δ is the Laplacian and $\nabla^i h = g^{ij} \partial_j h$ the gradient on \mathbb{S}^2 relative to the kinetic metric:

$$\Delta h = \left(\frac{1}{\sin^2 2\eta} \frac{\partial^2 h}{\partial \xi_2^2} + 2 \cot 2\eta \frac{\partial h}{\partial \eta} + \frac{\partial^2 h}{\partial \eta^2} \right) \quad \text{and} \quad |\nabla h|^2 = \frac{1}{\sin^2 2\eta} \left(\frac{\partial h}{\partial \xi_2} \right)^2 + \left(\frac{\partial h}{\partial \eta} \right)^2. \quad (34)$$

In fact we have an explicit formula for the scalar curvature, $R_{\mathbb{S}^2} = AB/C$ where

$$\begin{aligned} A &= 8 \sin^2 \eta ((\cos 2\eta + 2)^2 - 3 \sin^2 2\eta \cos^2 2\xi_2), \quad C = 3 (2 \sin^2 2\eta \cos 4\xi_2 + \cos 4\eta - 13)^3 \quad \& \\ B &= (-8 \sin^4 2\eta \cos 8\xi_2 - 16 \sin^2 2\eta \cos 4\xi_2 (\cos 4\eta - 29) + 236 \cos 4\eta - 3 \cos 8\eta + 727). \end{aligned} \quad (35)$$

As shown in [20], $R_{\mathbb{S}^2} \leq 0$ with equality only at Lagrange and collision points. Negativity of $R_{\mathbb{S}^2}$ also follows from (35): each factor in the numerator is ≥ 0 (the third vanishes at $L_{4,5}$, the second at $C_{1,2}$ and the first at C_3) while the denominator is strictly negative. We now use this to show that the scalar curvatures on configuration space \mathbb{C}^2 and its quotients \mathbb{R}^3 and \mathbb{S}^3 are strictly negative.

Scalar curvature on \mathbb{C}^2 : The equal-mass zero-energy JM metric on \mathbb{C}^2 from Eq. (11) is

$$ds_{\mathbb{C}^2}^2 = (Gm^3/r^2) h(\eta, \xi_2) (dr^2 + r^2 (d\eta^2 + d\xi_1^2 - 2 \cos 2\eta d\xi_1 d\xi_2 + d\xi_2^2)). \quad (36)$$

The scalar curvature of this metric is expressible as

$$R_{\mathbb{C}^2} = (3/2Gm^3 h^3) (4h^2 + |\nabla h|^2 - 2h \Delta h), \quad (37)$$

where Δh and ∇h are the Laplacian and gradient with respect to the *round* metric on \mathbf{S}^2 of radius one-half (34). Due to the scaling and rotation isometries, $R_{\mathbb{C}^2}$ is in fact a function on the shape sphere. The scalar curvatures on \mathbb{C}^2 (37) and \mathbb{S}^2 (33) are simply related:

$$R_{\mathbb{C}^2} = 3R_{\mathbb{S}^2} - (3/2Gm^3 h^3) (12h^2 + |\nabla h|^2). \quad (38)$$

This implies $R_{\mathbb{C}^2} < 0$ since the second term is strictly negative everywhere as we now show. Notice that the second term can vanish only when h is infinite, i.e., at collisions. Taking advantage of the fact that the geometry (on \mathbb{S}^2 and \mathbb{C}^2) in the neighborhood of all 3 collision points is the same for equal masses, it suffices to check that the second term has a strictly negative limit at C_3 ($\eta = 0$). Near $\eta = 0$, $h \sim 1/2\eta^2$ so that $R_{\mathbb{C}^2} \rightarrow -12/Gm^3 < 0$. Combining with the r -independence of $R_{\mathbb{C}^2}$, we see that the scalar curvature is non-singular at binary and triple collisions.

With a little more effort, we may obtain a non-zero upper bound for the Ricci scalar on \mathbb{C}^2 . Indeed, using $R_{\mathbb{S}^2} \leq 0$ and the inequality $12h^2 + |\nabla h|^2 \geq \zeta h^3$ proved in Appendix A, we find

$$R_{\mathbb{C}^2} < -3\zeta/2Gm^3 \quad \text{where} \quad \zeta = 55/27. \quad (39)$$

Numerically, we estimate the optimal value of ζ to be $8/3$.

Scalar curvatures on \mathbb{R}^3 and \mathbb{S}^3 : Recall that the equal-mass zero-energy quotient JM metrics on shape space \mathbb{R}^3 (17) and \mathbb{S}^3 (19) are

$$\begin{aligned} ds_{\mathbb{R}^3}^2 &= (Gm^3h/r^2) (dr^2 + r^2 (d\eta^2 + \sin^2 2\eta d\xi_2^2)) \quad \text{and} \\ ds_{\mathbb{S}^3}^2 &= Gm^3h (d\eta^2 + d\xi_1^2 - 2 \cos 2\eta d\xi_1 d\xi_2 + d\xi_2^2). \end{aligned} \quad (40)$$

The corresponding scalar curvatures are

$$R_{\mathbb{R}^3} = (16h^2 + 3|\nabla h|^2 - 4h\Delta h) / 2Gm^3h^3 \quad \text{and} \quad R_{\mathbb{S}^3} = (12h^2 + 3|\nabla h|^2 - 4h\Delta h) / 2Gm^3h^3. \quad (41)$$

Here Δh and ∇h are as in Eq. (34). The scalar curvatures are related to that on \mathbb{S}^2 as follows

$$R_{\mathbb{R}^3} = 2R_{\mathbb{S}^2} - (16h^2 + |\nabla h|^2) / 2Gm^3h^3 \quad \text{and} \quad R_{\mathbb{S}^3} = 2R_{\mathbb{S}^2} - (20h^2 + |\nabla h|^2) / 2Gm^3h^3. \quad (42)$$

As in the case of \mathbb{C}^2 we check that the second terms in both relations are strictly negative. This implies both the scalar curvatures are strictly negative. In fact, using the inequality $12h^2 + |\nabla h|^2 > \zeta h^3$ (see Appendix A) we find (non-optimal) non-zero upper bounds

$$R_{\mathbb{S}^3, \mathbb{R}^3} < -\zeta / 2Gm^3 \quad \text{where} \quad \zeta = 55/27. \quad (43)$$

Moreover, we note that

$$R_{\mathbb{C}^2} = R_{\mathbb{S}^3} - \frac{h\Delta h}{Gm^3h^3} < R_{\mathbb{S}^3} \quad \text{and} \quad R_{\mathbb{S}^3} = R_{\mathbb{R}^3} - \frac{4h^2}{2Gm^3h^3} \leq R_{\mathbb{R}^3}, \quad (44)$$

with equality at collision configurations. Recalling that on the shape sphere, the scalar curvature vanishes at collision points (in a limiting sense) and at Lagrange points, we have the following inequalities

$$0 \geq R_{\mathbb{S}^2} > R_{\mathbb{R}^3} \geq R_{\mathbb{S}^3} > R_{\mathbb{C}^2}. \quad (45)$$

Thus we have the remarkable result that the scalar curvatures of the JM metric on \mathbb{C}^2 and its quotients by scaling (\mathbb{S}^3) and rotations (\mathbb{R}^3) are strictly negative everywhere and also strictly less than that on \mathbb{S}^2 . So the full geodesic flow on \mathbb{C}^2 is in a sense more unstable than the corresponding flow on \mathbb{S}^2 .

In addition to strict negativity, we may also show that the scalar curvatures are bounded below. For instance, from Eq. (33) $R_{\mathbb{S}^2}$ can go to $-\infty$ only when $\Delta h \rightarrow \infty$ since $h \geq 3$. Now from Eq. (34) Δh can diverge only when $\sin 2\eta = 0$ or when one of the relevant derivatives of h diverges. From Eq. (12) this can happen only if $\eta = 0$ (C3) or $\eta = \pi/2$ (E3) or when one of the $v_i \rightarrow \infty$, i.e., at collisions. However $\Delta h = 66$ is finite at $\eta = \pi/2$ and we know from §3.3.1 that $R_{\mathbb{S}^2}$ is finite at collisions so that $R_{\mathbb{S}^2}$ is bounded below. The same proof shows that scalar curvatures are bounded below on $\mathbb{R}^3, \mathbb{S}^3$ and \mathbb{C}^2 as well.

3.5 Sectional curvature for three equal masses

In §3.4, we showed that the Ricci scalars R on configuration space and its quotients are negative everywhere, save at Lagrange and collision points on the shape sphere where it vanishes. However, R encodes the stability of geodesics only in an average sense. More precisely, a geodesic through P in the direction u subject to a perturbation along v is linearly stable/unstable according as the sectional curvature $K_P(u, v)$ is positive/negative (see §3.6). Here,

the sectional curvature which is a function only of the 2-plane spanned by u and v generalizes the Gaussian curvature to higher dimensions. It is defined as the ratio of the curvature biquadratic $\kappa = g(R(u, v)v, u)$ to the square of the area $\text{Ar}(u, v)^2 = g(u, u)g(v, v) - g(u, v)g(v, u)$ of the parallelogram spanned by u and v . Here $g(u, v)$ is the Riemannian inner product and $R(u, v) = [\nabla_u, \nabla_v] - \nabla_{[u, v]}$ the curvature tensor with components $R(e_i, e_j)e_k = R^l_{kij}e_l$ in any basis for vector fields. Furthermore, if e_1, \dots, e_n are an orthonormal basis for the tangent space at P , then the scalar curvature $R = \sum_{i \neq j} K(e_i, e_j)$ is the sum of sectional curvatures in $\binom{n}{2}$ planes through P . It may also be regarded as an average of the curvature biquadratic $R = \iint \kappa(u, v) d\mu_g(u) d\mu_g(v)$ where $d\mu_g(u) = \exp(-u^i u^j g_{ij}/2) du$ is the gaussian measure on tangent vectors with mean zero and covariance g^{ij} [31]. Thus R provides an averaged notion of stability. To get a more precise measure of linear stability of geodesics we find the sectional curvatures in various (coordinate) tangent 2-planes of the configuration space and its quotients. On account of the isometries, these sectional curvatures are functions only of η and ξ_2 [explicit expressions are omitted due to their length]. Unlike scalar curvatures which were shown to be non-positive, we find planes in which sectional curvatures are non-positive as well as planes where they can have either sign.

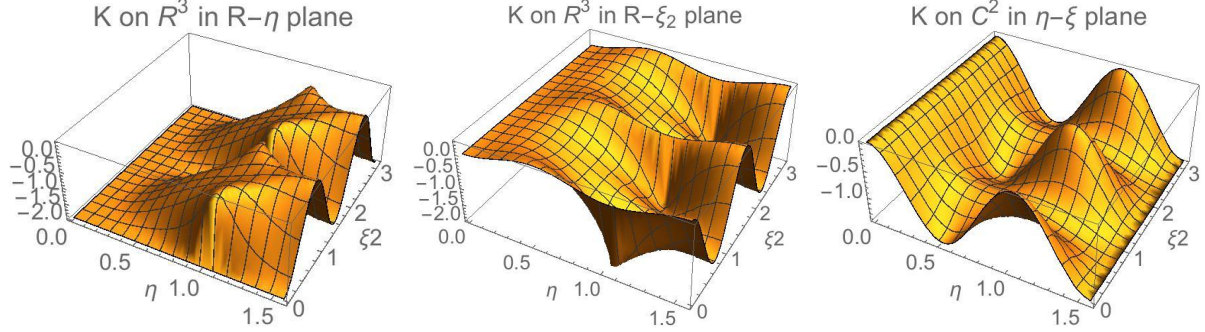
O'Neill's theorem allows us to determine or bound certain sectional curvatures on the configuration space \mathbb{C}^2 in terms of the more easily determined curvatures on its quotients. Roughly, the sectional curvature of a horizontal two-plane increases under a Riemannian submersion. Suppose $f : (M, g) \rightarrow (N, \tilde{g})$ is a Riemannian submersion. Then O'Neill's theorem [29] states that the sectional curvature in any horizontal 2-plane at $m \in M$ is less than or equal to that on the corresponding 2-plane at $f(m) \in N$:

$$K_N(df(X), df(Y)) = K_M(X, Y) + \frac{3 |[X, Y]^V|^2}{4 \text{Ar}(X, Y)^2}. \quad (46)$$

Here X and Y are horizontal fields on M spanning a non-degenerate 2-plane ($\text{Ar}(X, Y)^2 \neq 0$) and $[X, Y]^V$ is the vertical projection of their Lie bracket. In particular, the sectional curvatures are equal everywhere if X and Y are coordinate vector fields.

We consider sectional curvatures in 6 interesting 2 planes on \mathbb{C}^2 which are horizontal with respect to submersions to \mathbb{R}^3 and \mathbb{S}^3 . Under the submersion from \mathbb{C}^2 to \mathbb{R}^3 (§3.2), the horizontal basis vectors ∂_r , ∂_η and $\partial_\xi \equiv \cos 2\eta \partial_{\xi_1} + \partial_{\xi_2}$ map respectively to ∂_r , ∂_η and ∂_{ξ_2} defining three pairs of corresponding 2-planes. Since $[\partial_r, \partial_\eta]$ and $[\partial_r, \partial_\xi]$ vanish, we have $K_{\mathbb{C}^2}(\partial_r, \partial_\eta) = K_{\mathbb{R}^3}(\partial_r, \partial_\eta)$ and $K_{\mathbb{C}^2}(\partial_r, \partial_\xi) = K_{\mathbb{R}^3}(\partial_r, \partial_{\xi_2})$. Fig. 4 shows that $K_{\mathbb{C}^2}(\partial_r, \partial_\eta)$ is mostly negative, though it is not continuous at E_3 , C_1 and C_2 . On the other hand $K_{\mathbb{C}^2}(\partial_r, \partial_\xi)$ is largely negative except in a neighbourhood of C_3 . Finally, as $[\partial_\xi, \partial_\eta]^V = -2 \sin 2\eta \partial_{\xi_1} \neq 0$, we have $K_{\mathbb{C}^2}(\partial_\eta, \partial_\xi) < K_{\mathbb{R}^3}(\partial_\eta, \partial_{\xi_2})$ with equality at collisions. Moreover the submersion from $\mathbb{R}^3 \rightarrow \mathbb{S}^2$ (§3.2) implies that $K_{\mathbb{R}^3}(\partial_\eta, \partial_{\xi_2})$ coincides with $K_{\mathbb{S}^2}(\partial_\eta, \partial_{\xi_2})$ which vanishes at Lagrange and collision points and is strictly negative elsewhere (see §3.4). Thus $K_{\mathbb{C}^2}(\partial_\eta, \partial_\xi)$ vanishes at collision points and is strictly negative everywhere else (see Fig. 4). In particular, Lagrange points are more unstable on the configuration space \mathbb{C}^2 than on the shape sphere.

Under the submersion from \mathbb{C}^2 to \mathbb{S}^3 (§3.2), the horizontal basis vectors ∂_η , ∂_{ξ_1} and ∂_{ξ_2} map respectively to ∂_η , ∂_{ξ_1} and ∂_{ξ_2} . The sectional curvatures on corresponding pairs of 2-planes are equal, e.g. $K_{\mathbb{C}^2}(\partial_\eta, \partial_{\xi_2}) = K_{\mathbb{S}^3}(\partial_\eta, \partial_{\xi_2})$. As shown in Fig. 5, $K_{\mathbb{C}^2}(\partial_\eta, \partial_{\xi_2})$ is negative everywhere except in a neighbourhood of E_3 where it can have either sign. The qualitative behavior of the other two sectional curvatures $K_{\mathbb{C}^2}(\partial_{\xi_1}, \partial_{\xi_2})$ and $K_{\mathbb{C}^2}(\partial_{\xi_1}, \partial_\eta)$ is similar to that



- (a) $K_{\mathbb{C}^2}(\partial_r, \partial_\eta) = K_{\mathbb{R}^3}(\partial_r, \partial_\eta) \leq 0$ everywhere except in neighborhoods of E_3 . $K = -2$ at its global minimum C_3 and $K = -2/3$ at $L_{4,5}$. $K \rightarrow 0, -2$ when $C_{1,2}$ are approached holding η or ξ_2 fixed.
- (b) $K_{\mathbb{C}^2}(\partial_r, \partial_{\xi_2}) = K_{\mathbb{R}^3}(\partial_r, \partial_{\xi_2})$ is negative except in neighborhoods of C_3 and E_3 . $K = 0$ at its minimum C_3 ($\eta = 0$) and $K = -2/3$ at $L_{4,5}$. $K \rightarrow -2$ or 0 on approaching $C_{1,2}$ ($\eta = \pi/3, \xi_2 = 0, \pi/2$) along η or ξ_2 constant.
- (c) $K_{\mathbb{C}^2}(\partial_\eta, \partial_\xi) \leq K_{\mathbb{R}^3}(\partial_\eta, \partial_{\xi_2})$. $K_{\mathbb{C}^2}(\partial_\eta, \partial_\xi) = 0$ at global maxima $C_{1,2,3}$ and is negative elsewhere. $K = -1$ at its local maxima $L_{4,5}$.

Figure 4: Sectional curvatures on horizontal 2-planes of submersion from \mathbb{C}^2 to \mathbb{R}^3 in units of $1/Gm^3$.

of $K_{\mathbb{C}^2}(\partial_r, \partial_{\xi_2})$ and $K_{\mathbb{C}^2}(\partial_r, \partial_\eta)$ discussed above. The approximate symmetry under $\partial_{\xi_1} \leftrightarrow \partial_r$ is not entirely surprising given that ∂_{ξ_1} and ∂_r are vertical vectors in the submersions to \mathbb{R}^3 and \mathbb{S}^3 respectively.

The remaining two coordinate 2-planes on \mathbb{C}^2 are not horizontal under either submersion. We find that $K_{\mathbb{C}^2}(\partial_r, \partial_{\xi_1})$ is negative everywhere except at $L_{4,5}$ and $K_{\mathbb{C}^2}(\partial_r, \partial_{\xi_2})$ is negative except around $E_{1,2}$.

3.6 Stability tensor and linear stability of geodesics

In this section we use the stability tensor (which provides a criterion for linear geodesic stability) to discuss the stability of Lagrange rotational and homothety solutions. We end with a remark on linear stability of trajectories and geodesics. Consider the n -dimensional configuration manifold M with metric g . The geodesic deviation equation (GDE) for the evolution of the separating vector (Jacobi field) $y(t)$ between a geodesic $x(t)$ and a neighboring geodesic is [29]

$$\nabla_{\dot{x}}^2 y = R(\dot{x}, y)\dot{x} = -R(y, \dot{x})\dot{x}. \quad (47)$$

We expand the Jacobi field $y = c^k(t)e_k(t)$ in any basis $e_i(t)$ that is parallel transported along the geodesic i.e. $\nabla_{\dot{x}} e_k = 0$ [$e_i(0)$ could be taken as coordinate vector fields at $x(0)$]. Taking the inner product of the GDE with e_m and contracting with g^{im} , we get $\ddot{c}^i = -S_j^i c^j$, where the ‘stability tensor’ $S_k^i = R_{jkl}^i \dot{x}^j \dot{x}^l$. As S is real symmetric, its eigenvectors f_i can be chosen to form an orthonormal basis for $T_x M$. Writing $y = d^m f_m$, the GDE becomes $\ddot{d}^m = -\kappa_m d^m$ (no sum on m) where κ_m is the eigenvalue of S corresponding to the eigenvector f_m . The eigenvalues of S (say at $t = 0$) control the initial evolution of the Jacobi fields in the corresponding eigendirections. Since $\kappa_m = (\text{Area}\langle f_k, \dot{x} \rangle)^2 K(f_m, \dot{x})$ (§3.5), positive (negative) κ or

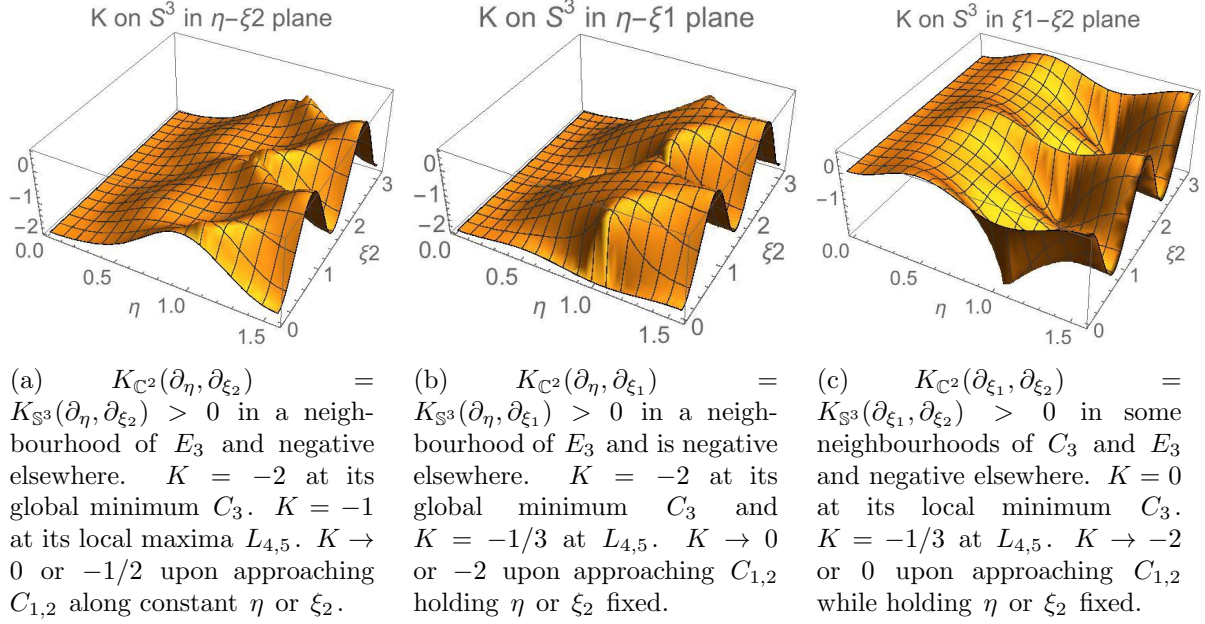


Figure 5: Sectional curvatures on horizontal 2-planes of submersion from \mathbb{C}^2 to \mathbb{S}^3 in units of $1/Gm^3$.

K imply local stability (instability) for the initial evolution. We note that calculating S and its eigenvalues at a given instant (say $t = 0$) requires no knowledge of the time evolution of $e_i(t)$. So we may simply use the coordinate vector fields as the basis. Notice that the tangent vector to the geodesic \dot{x} is always an eigendirection of S with eigenvalue zero.

Rotational Lagrange solutions in Newtonian potential: Consider the Lagrange rotational solutions where three equal masses ($m_i = m$) rotate at angular speed $\omega = \sqrt{3Gm/a^3}$ around their CM at the vertices of an equilateral triangle of side a . The rotational trajectory on \mathbb{C}^2 in $r, \eta, \xi_{1,2}$ coordinates is given by $x(t) = (a/\sqrt{m}, \pi/4, \omega t, \pm\pi/4)$ with velocity vector $\omega\partial_{\xi_1}$. Note that trajectory and geodesic times are proportional since $\sigma = ds/dt = (E - V)/\sqrt{\mathcal{T}}$ with $V(r, \eta, \xi_2)$ and \mathcal{T} constant along $x(t)$. The stability tensor along the geodesic, $S = \omega^2 \text{diag}(1, -1/2, 0, -1/2)$ is diagonal in the coordinate basis r, η, ξ_1, ξ_2 . As always, \dot{x} is a zero-mode. A perturbation along ∂_r is linearly stable while those directed along ∂_η or ∂_{ξ_2} are linearly unstable. Note that Routh's criterion $27(m_1m_2 + m_2m_3 + m_3m_1) < M^2$ [3] predicts that Lagrange rotational solutions are linearly unstable for equal masses.

Lagrange homotheties: For equal masses, a Lagrange homothety solution is one where the masses move radially (towards/away from their CM) while being at the vertices of equilateral triangles. The geodesic in Hopf coordinates takes the form $(r(t), \eta = \pi/4, \xi_1, \xi_2 = \pm\pi/4)$ where ξ_1 is arbitrary and independent of time. Though an explicit expression is not needed here, $r(t)$ is the solution of $\ddot{r} + \Gamma_{rr}^r \dot{r}^2 = 0$ where $\Gamma_{rr}^r = -3Gm^3/(Er^3 + 3Gm^3r)$ for the inverse-square potential. The stability tensor is diagonal:

$$S = \frac{6Gm^3\dot{r}^2}{(3Gm^3r + Er^3)^2} \text{diag}(0, -3Gm^3 - 2Er^2, -Er^2, -3Gm^3 - 2Er^2). \quad (48)$$

For a given r and positive energy, perturbations along $\partial_{\xi_{1,2}}$ and ∂_η are unstable while they are stable when $-3Gm^3/r^2 < E < -3Gm^3/2r^2$. For intermediate (negative) energies, ∂_η and

∂_{ξ_2} are unstable directions while ∂_{ξ_1} is stable. For the Newtonian potential, we have similar conclusions following from the corresponding stability tensor:

$$S = \frac{3Gm^{5/2}\dot{r}^2}{4r^2(3Gm^{5/2} + Er)^2} \text{diag} \left(0, -9Gm^{5/2} - 5Er, -2Er, -9Gm^{5/2} - 5Er \right). \quad (49)$$

We end this section with a cautionary remark. For a system whose trajectories can be regarded as geodesics of the JM metric, linear stability of geodesics may not coincide with linear stability of corresponding trajectories. This may be due to the reparametrization of time (see §3.3.2 for examples) as well as the restriction to energy conserving perturbations in the GDE. We illustrate this with a 2D isotropic oscillator with spring constant k . Here the curvature of the JM metric (see §2) is $R = 2Ek/T^3$ where T is the kinetic energy. Thus for positive k , geodesics are always linearly stable while for negative k they are stable/unstable according as energy is negative/positive. By contrast, linearizing the EOM $\ddot{x}_i = -(k/m)\delta x_i$ shows that trajectories are linearly stable for positive k and linearly unstable for negative k . This (possibly atypical) example illustrates the fact that geodesic stability does not necessarily imply stability of trajectories.

4 Planar three-body problem with Newtonian potential

4.1 JM metric and its curvature on configuration and shape space

In analogy with our geometric treatment of the planar motion of three masses subject to inverse-square potentials, we briefly discuss the gravitational analogue with Newtonian potentials. As before, the translation invariance of the Lagrangian

$$L = \frac{1}{2} \sum_{i=1,2,3} m_i \dot{x}_i^2 - \sum_{i<j} \frac{Gm_i m_j}{|x_i - x_j|} \quad (50)$$

allows us to go from the configuration space \mathbb{C}^3 to its quotient \mathbb{C}^2 endowed with the JM metric

$$ds^2 = \left(E + \frac{Gm_1 m_2}{|J_1|} + \frac{Gm_2 m_3}{|J_2 - \mu_1 J_1|} + \frac{Gm_3 m_1}{|J_2 + \mu_2 J_1|} \right) (M_1 |dJ_1|^2 + M_2 |dJ_2|^2). \quad (51)$$

The Jacobi coordinates $J_{1,2}$, mass ratios $\mu_{1,2}$ and reduced masses $M_{1,2}$ are as defined in Eqs. (5, 6, 7). In rescaled Jacobi coordinates $z_i = \sqrt{M_i} J_i$ (8), the JM metric on \mathbb{C}^2 for *equal masses* becomes

$$ds^2 = \left(E + \frac{Gm^{5/2}}{\sqrt{2}|z_1|} + \frac{\sqrt{2}Gm^{5/2}}{\sqrt{3}|z_2 - \frac{1}{\sqrt{3}}z_1|} + \frac{\sqrt{2}Gm^{5/2}}{\sqrt{3}|z_2 + \frac{1}{\sqrt{3}}z_1|} \right) (|dz_1|^2 + |dz_2|^2). \quad (52)$$

Rotations $z_j \mapsto e^{i\theta} z_j$ continue to act as isometries corresponding to the KVF ∂_{ξ_1} in Hopf coordinates (10), where the JM metric is

$$\begin{aligned} ds^2 &= \left(E + Gm^{5/2}U/r \right) (dr^2 + r^2 (d\eta^2 + d\xi_1^2 - 2 \cos 2\eta d\xi_1 d\xi_2 + d\xi_2^2)) \quad \text{with} \\ U &= \frac{1}{\sqrt{2} \sin \eta} + \frac{\sqrt{2}}{\sqrt{2 + \cos 2\eta - \sqrt{3} \sin 2\eta \cos 2\xi_2}} + \frac{\sqrt{2}}{\sqrt{2 + \cos 2\eta + \sqrt{3} \sin 2\eta \cos 2\xi_2}}. \end{aligned} \quad (53)$$

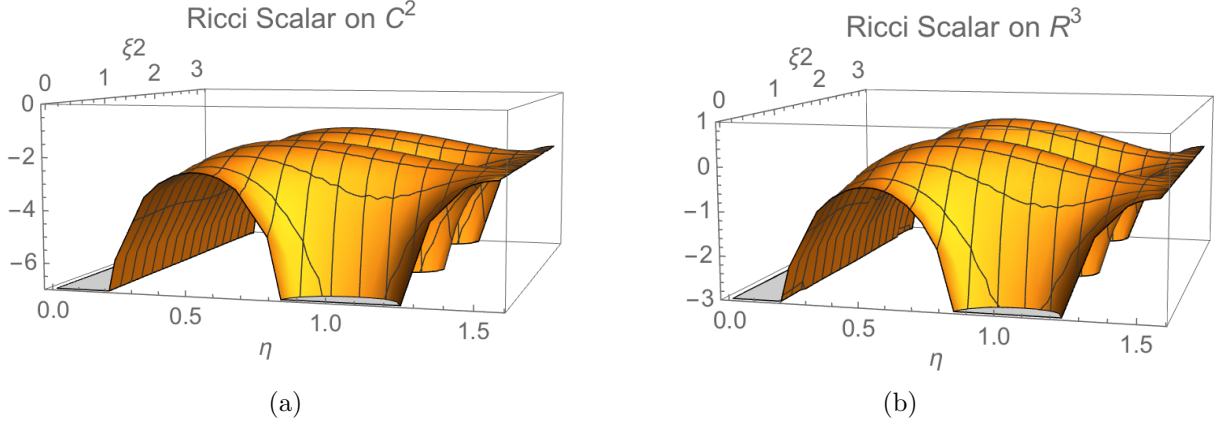


Figure 6: Ricci scalar R for zero energy and equal masses on \mathbb{C}^2 and \mathbb{R}^3 for the Newtonian potential (in units of $1/Gm^{5/2}r$). R on \mathbb{C}^2 is strictly negative while that on \mathbb{R}^3 can have either sign.

Requiring the submersion $(r, \eta, \xi_1, \xi_2) \mapsto (r, \eta, \xi_2)$ from \mathbb{C}^2 to its quotient by rotations to be Riemannian gives us the JM metric on shape space \mathbb{R}^3 :

$$ds^2 = \left(E + Gm^{5/2}U/r \right) \left(dr^2 + r^2 (d\eta^2 + \sin^2 2\eta d\xi_2^2) \right). \quad (54)$$

Unlike for the inverse-square potential, scaling $r \mapsto \lambda r$ is not an isometry of the JM metric even when $E = 0$. Thus we do not have a further submersion to the shape sphere. However, in what follows, we will consider $E = 0$, as it leads to substantially simpler curvature formulae.

Though we do not have a submersion to the shape sphere, the quantity $U(\eta, \xi_2)$ in the conformal factor may be regarded as a function on a 2-sphere of radius one-half. This allows us to express the scalar curvatures as

$$R_{\mathbb{C}^2} = \frac{3}{2Gm^{5/2}rU^3} (3U^2 + |\nabla U|^2 - 2U\Delta U) \quad \text{and} \quad R_{\mathbb{R}^3} = \frac{1}{4Gm^{5/2}rU^3} (30U^2 + 6|\nabla U|^2 - 8U\Delta U) \quad (55)$$

where ΔU is the Laplacian and ∇U the gradient relative to the round metric on a 2-sphere of radius $1/2$. Evidently, both the scalar curvatures vanish in the limit $r \rightarrow \infty$ of large moment of inertia $I_{\text{CM}} = r^2$; they are plotted in Fig. 6. Numerically, we find that for any fixed r , $R_{\mathbb{C}^2}$ is strictly negative and reaches its global maximum $-3/(2Gm^{5/2}r)$ at the Lagrange configurations $L_{4,5}$, while $R_{\mathbb{R}^3}$ has a positive global maximum $1/(2Gm^{5/2}r)$ at the same locations. Note that $R_{\mathbb{R}^3} = 2R_{\mathbb{C}^2}/3 + (9U^2 + |\nabla U|^2)/(2Gm^{5/2}rU^3)$. As argued in Eq. (38), the second term is strictly positive and vanishes only when $r \rightarrow \infty$. Using the negativity of $R_{\mathbb{C}^2}$, it follows that $R_{\mathbb{R}^3} > R_{\mathbb{C}^2}$ with $(R_{\mathbb{R}^3} - R_{\mathbb{C}^2})$ attaining its minimum $2/(Gm^{5/2}r)$ at $L_{4,5}$. Thus in a sense, the geodesic dynamics on \mathbb{C}^2 is more linearly unstable than on shape space. Like the Ricci scalars, sectional curvatures on coordinate 2-planes are $(1/r) \times$ a function of η and ξ_2 . We find that sectional curvatures are largely negative and often go to $\pm\infty$ at collision points (see Eq. (57)).

4.2 Near-collision geometry and ‘geodesic incompleteness’

Unlike for the inverse-square potential, the scalar curvatures on \mathbb{C}^2 and \mathbb{R}^3 (55) diverge at binary and triple collisions. To examine the geometry near pairwise collisions of equal masses, it

suffices to study the geometry near C_3 ($\eta = 0$, $r \neq 0$, $\xi_{1,2}$ arbitrary) which represents a collision of m_1 and m_2 . We do so by retaining only those terms in the expansion of the zero-energy metrics around $\eta = 0$:

$$\begin{aligned} ds_{\mathbb{C}^2}^2 &\approx \left(Gm^{5/2}/\sqrt{2}\eta r \right) (dr^2 + r^2 (d\eta^2 + d\xi_1^2 - 2(1-2\eta^2)d\xi_1 d\xi_2 + d\xi_2^2)) \quad \text{and} \\ ds_{\mathbb{R}^3}^2 &\approx \left(Gm^{5/2}/r \right) \left(1/\sqrt{2}\eta + 2\sqrt{2/3} \right) (dr^2 + r^2 (d\eta^2 + 4\eta^2 d\xi_2^2)), \end{aligned} \quad (56)$$

that are necessary to arrive at the following curvatures to leading order in η :

$$\begin{aligned} \text{on } \mathbb{C}^2: \quad R &= -3/\varrho \quad \text{and} \quad K(\partial_\eta, \partial_{r,\xi_{1,2}}) = 2K(\partial_r, \partial_{\xi_{1,2}}) = -2K(\partial_{\xi_1}, \partial_{\xi_2}) = -1/\varrho \\ \text{on } \mathbb{R}^3: \quad R &= -1/\varrho \quad \text{and} \quad K(\partial_\eta, \partial_r) = -2K(\partial_r, \partial_{\xi_2}) = -1/\varrho, \quad K(\partial_\eta, \partial_{\xi_2}) = -\frac{2\sqrt{2/3}}{Gm^{5/2}} \end{aligned} \quad (57)$$

where $\varrho = \sqrt{2}Gm^{5/2}\eta r$. The curvature singularity at $\eta = 0$ is evident in the simple poles in the Ricci scalars and all but one of the sectional curvatures in coordinate planes.

We use the near-collision JM metric of Eq. (56) to show that a pairwise collision point lies at finite geodesic distance from another point in its neighborhood. Thus, unlike for the inverse-square potential, the geodesic reformulation *does not* regularize the gravitational three-body problem. Consider a point P near $\eta = 0$ with coordinates $(r, \eta_0, \xi_1, \xi_2)$. We estimate its distance to the collision point C_3 $(r, 0, \xi_1, \xi_2)$. To do so, we consider a curve γ of constant r , ξ_1 and ξ_2 running from P to C_3 parametrized by $\eta_0 \geq \eta \geq 0$. We will show that γ has finite length so that the geodesic distance to C_3 must be finite. In fact, from (56):

$$\text{Length}(\gamma) = \int_{\eta_0}^0 \sqrt{\frac{Gm^{5/2}}{\sqrt{2}}} \frac{d\eta}{\sqrt{\eta}} = -2\sqrt{\frac{Gm^{5/2}}{\sqrt{2}}} \sqrt{\eta_0} < \infty. \quad (58)$$

Furthermore, the image of γ under the Riemannian submersion to shape space \mathbb{R}^3 is a curve of even shorter length ending at a collision point. Thus geodesics on \mathbb{C}^2 and \mathbb{R}^3 can reach binary collisions in finite time, where the scalar curvature is singular. It is therefore interesting to study regularizations of collisions in the three body problem and their geometric interpretation.

Acknowledgements: We thank K G Arun, A Lakshminarayan, R Montgomery, S G Rajeev and A Thyagaraja for useful discussions and references. This work was supported in part by the Infosys Foundation and a Ramanujan grant of the Department of Science & Technology, Govt. of India.

A Proof of an inequality to give an upper bound for the scalar curvature

Here we establish a strict lower bound on the quantity that appears in the relation (38) between Ricci scalars on \mathbb{C}^2 and \mathbb{S}^2 . Since Montgomery has shown that $R_{\mathbb{S}^2} \leq 0$, this helps us establish strictly negative upper bounds for the scalar curvatures on \mathbb{C}^2 , \mathbb{R}^3 and \mathbb{S}^3 . We will show here that

$$12h^2 + |\nabla h|^2 > \zeta h^3 \quad \text{where} \quad \zeta = 55/27 \approx 2.04. \quad (59)$$

The best possible ζ is estimated numerically to be $\zeta = 8/3$ and the minimum occurs at the Euler points $E_{1,2,3}$. We define the power sum symmetric functions $u_{2n} = \sum_{i=1}^3 v_i^n$ in terms of

which the pre-factor in the JM metric (12) is $h = v_1 + v_2 + v_3 = u_2$. In [20] Montgomery shows that $|\nabla h|^2 = 4s$ where the symmetric polynomial

$$s = (1/2) (-2u_2^2 + 4u_2u_4 - 3u_4^2 + 3u_8). \quad (60)$$

This gives

$$12h^2 + |\nabla h|^2 = u_2^3 (8A + 6B) \quad \text{where} \quad A = \frac{u_2 + u_4}{u_2^2} \quad \text{and} \quad B = \frac{u_8 - u_4^2}{u_2^3}. \quad (61)$$

We will show below that $A \geq 17/27$ and $B > -1/2$, from which Eq. (59) follows (numerically we find that $B \geq -32/81$ which leads to the above-mentioned optimal value $\zeta = 8/3$). To prove the inequality for B , we define $c = \cos 2\eta$ and $s = \sin 2\eta \cos 2\xi_2$ which lie in the interval $[-1, 1]$. Then

$$\frac{u_8 - u_4^2}{u_2^3} > -\frac{1}{2} \quad \Leftrightarrow \quad u_8 - u_4^2 + \frac{u_2^3}{2} > 0 \quad \Leftrightarrow \quad \frac{3}{8} (20 - 3(c^2 + s^2)^2 - 8c^3 + 24cs^2) > 0. \quad (62)$$

For the latter to hold it is sufficient that $17 - 8c^3 + 24cs^2 > 0$ which is clearly true for $0 \leq c \leq 1$. For $-1 \leq c < 0$ put $c = -d$. Then it is enough to show that $17 + 8d^3 - 24d(1 - d^2) > 0$ since $s^2 \leq 1 - d^2$. This holds as the LHS is positive at its boundary points $d = 0, 1$ as well as at its local extremum $d = 1/2$.

The quantity A defined in Eq. (61) is a symmetric function of v_1, v_2 and v_3 which in turn are functions of η and ξ_2 (12) for $0 \leq \eta \leq \pi/2$ and $0 \leq \xi_2 \leq \pi$. Since $\sum_i 1/v_i = 3$, we may regard A as a function of any pair, say v_1 and v_2 . The allowed values of η and ξ_2 define a domain $\bar{D} = D \cup \partial D$ in the v_1 - v_2 plane. To show that $A \geq 17/27$, we seek its global minimum, which must lie either at a local extremum in the interior D or on the boundary ∂D . ∂D is defined by the curves $\xi_2 = 0$ and $\xi_2 = \pi/2$ which meet at $\eta = 0$ and $\eta = \pi/2$ and include the points $(v_1 = \infty, v_2 = 2/3)$ and $(v_1 = 2/3, v_2 = \infty)$ (see Fig. 7). This is because, for any fixed η , v_1 and v_2 (12) are monotonic functions of ξ_2 for $0 \leq \xi_2 \leq \pi/2$ and symmetric under reflection about $\xi_2 = \pi/2$. Along ∂D , $A = (5 \cos 6\eta + 22)/27$ is independent of ξ_2 and minimal at the Euler configurations $\eta = \pi/6$ and $\pi/2$ with the common minimum value $17/27$, which turns out to be the global minimum of A . This is because its only local extremum in D is at the Lagrange configuration $v_1 = v_2 = v_3 = 1$ where $A = 2/3$. To see this, we note that local extrema of A in D must lie at the intersections of $\partial A/\partial v_1 = 0$ and $\partial A/\partial v_2 = 0$. Now $\partial A/\partial v_1 = (v_1 - v_3)F(v_1, v_2)/v_1^2 u_2^3$ where

$$F(v_1, v_2) = u_2 \{v_1 + v_3 + 2(v_1^2 + v_1 v_3 + v_3^2)\} - 2(v_1 + v_3)(u_2 + u_4). \quad (63)$$

For $\partial A/\partial v_1$ to vanish, either $v_1 = v_3$ or $F(v_1, v_2) = 0$ or one of the $v_i = \infty$. The collision points $v_i = \infty$ do not lie in D . The conditions for $\partial A/\partial v_2$ to vanish are obtained via the exchange $v_1 \leftrightarrow v_2$. The intersection of the conditions $v_1 = v_3$ and $v_2 = v_3$ lies at the Lagrange configurations $v_i = 1$ where $A = 2/3$. It turns out that the only intersection of $v_1 = v_3$ with $F(v_2, v_1) = 0$ or of $v_2 = v_3$ with $F(v_1, v_2) = 0$ lying in D occurs at the above Lagrange configuration. For instance, when $v_1 = v_3 = v$, $F(v_2, v_1) = -3v^2(4v - 1)(v - 1)/(3v - 2)^2$ vanishes when $v = 1$ or $v = 1/4$ (which violates $v \geq 1/2$). Finally, we account for extrema lying on the zero loci of both $F(v_1, v_2)$ and $F(v_2, v_1)$, which using $u_{-2} = 3$, must satisfy

$$F(v_1, v_2) - F(v_2, v_1) = (v_1 - v_2) [12v_1 v_2 v_3 - (v_1 + v_2 + v_3)] = 0. \quad (64)$$

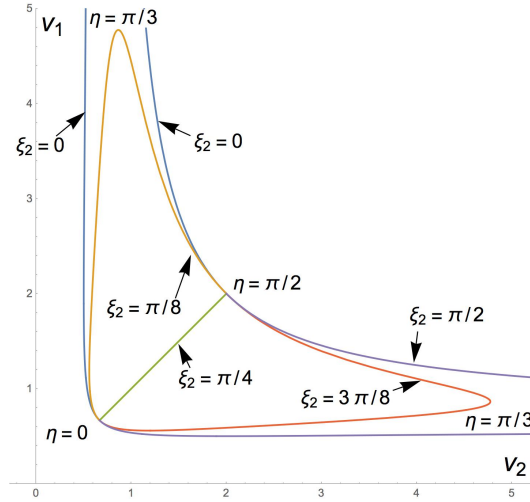


Figure 7: The boundary ∂D of the region D in the v_1 - v_2 plane is given by the level curves $\xi_2 = 0, \pi/2$. These level curves run from the collision point $\eta = 0$ to the Euler point $\eta = \pi/2$, passing through the collision points at $v_1 = \infty$ or $v_2 = \infty$ (where $\eta = \pi/3$). The level curves $\xi_2 = \pi/8, \pi/4, 3\pi/8$ in the interior D are also shown. Note that D lies within the quadrant $v_{1,2} \geq 1/2$.

So either $v_1 = v_2$ or $12v_1v_2v_3 = u_2$. Now, we have shown above that the only extrema of A on $v_1 = v_3$ in D lie at the Lagrange configurations. Since A is a symmetric function of the v_i , it follows that its only extrema on $v_1 = v_2$ also lies at the Lagrange configurations. On the other hand, $12v_1v_2v_3 - (v_1 + v_2 + v_3) \geq 0$ for $v_i \geq 1/2$, with equality only at $v_i = 1/2$ which is not in D . Thus the only extremum of A in D is at the Lagrange configurations (where $A = 2/3$) and hence its global minimum occurs on ∂D at the Euler configurations (where $A = 17/27$).

References

- [1] Gutzwiller, M. C., *Moon-Earth-Sun: The oldest three-body problem*, Reviews of Modern Physics, **70**, 589 (1998).
- [2] Chenciner, A., *Poincaré and the Three-Body Problem in Henri Poincaré, 1912-2012, Poincaré Seminar 2012*, Eds. Duplantier B. and Rivasseau V., Springer, Basel (2015).
- [3] Routh, E. J., *A Treatise on the Stability of a Given State of Motion: Particularly Steady Motion*, Macmillan (1877).
- [4] Laskar, J., *Is the Solar System stable?* Progress in Mathematical Physics, **66**, 239-270 (2013).
- [5] Montgomery, R., *A new solution to the three-body problem*, Notices of Amer. Math. Soc., **48**, No. 5, 471-481 (2001).
- [6] Gutzwiller, M. C., *Chaos in Classical and Quantum mechanics*, Vol. 1, Interdisciplinary Applied Mathematics, Springer-Verlag, New York (1990).
- [7] Newton, P. K., *The N-Vortex Problem: Analytical Techniques*, Springer-Verlag, New York, (2001).
- [8] Efimov, V., *Energy levels arising from resonant two-body forces in a three-body system*, Physics Letters B, **33**, 563 (1970).
- [9] Kraemer, T., Mark, M., Waldburger, P., Danzl, J. G., Chin, C., Engeser, B., Lange, A. D., Pilch, K., Jaakkola, A., Nagerl, H.-C. and Grimm, R., *Evidence for Efimov quantum states in an ultracold gas of caesium atoms*, Nature, **440**, 315 (2006).

- [10] Calogero, F., *Solution of a three-body problem in one dimension*, J. Math. Phys., **10**, 2191 (1969).
- [11] Rajeev, S. G., *Advanced Mechanics: From Euler's Determinism to Arnold's Chaos*, Oxford Univ Press (2013).
- [12] Lanczos, C., *The variational principles of mechanics*, 4th ed. Dover (1970), page 139.
- [13] Arnold, V. I., *Mathematical Methods of Classical Mechanics*, 2nd ed., Springer Verlag (1989), page 245.
- [14] Casetti, L., Pettini, M. and Cohen, E. G. D., *Geometric approach to Hamiltonian dynamics and statistical mechanics*, Physics Reports, **337**, 237 (2000). arXiv:cond-mat/9912092.
- [15] Pettini M. *Geometry and Topology in Hamiltonian Dynamics and Statistical Mechanics*, Springer (2007), chapter 3.
- [16] Cerruti-Sola, M., Ciruolo, G., Franzosi, R. and Pettini, M., *Riemannian geometry of Hamiltonian chaos: Hints for a general theory*, Phys. Rev. E, **78**, 046205 (2008).
- [17] Cerruti-Sola, M. and Pettini M., *Geometric description of chaos in two-degrees-of-freedom Hamiltonian systems*, Phys. Rev. E, **53**, 179 (1996).
- [18] Ramasubramanian, K. and Sriram, M. S., *Global geometric indicator of chaos and Lyapunov exponents in Hamiltonian systems*, Phys. Rev. E, **64**, 046207 (2001).
- [19] Montgomery, R., *The Three-body problem and the shape sphere*, The American Mathematical Monthly, **122**, 299-321 (2015).
- [20] Montgomery, R., *Hyperbolic pants fit a three-body problem*, Ergodic Theory and Dynamical Systems, **25**, 921-947 (2005).
- [21] Montgomery, R., *Infinitely Many Syzygies*, Archives for Rational Mechanics, **164**, 311 (2002).
- [22] Montgomery, R., *The zero angular momentum three-body problem: all but one solution has syzygies*, Ergodic Theory and Dynamical Systems, **27**, 1933 (2007).
- [23] Chenciner, A., *Three Body Problem*, Scholarpedia, 2(10):2111 (2007).
- [24] Moore, C., *Braids in classical dynamics*, Phys. Rev. Lett., **70**, 3675 (1993).
- [25] Montgomery, R., *The N-body problem, the braid group, and action-minimizing periodic solutions*, Nonlinearity, **11**, 363 (1998).
- [26] Chenciner, A., *Action minimizing solutions of the Newtonian n-body problem: from homology to symmetry*, Proceedings of the ICM, Beijing, **3**, 255-264, World Scientific (2002).
- [27] Yeomans, D. K., *Exposition of Sundman's regularization of the three-body problem*, NASA Goddard Space Flight Center Technical Report, NASA-TM-X-55636, X-640-66-481 (1966).
- [28] Celletti, A., *Basics of Regularization Theory*, in *Chaotic Worlds: From Order to Disorder in Gravitational N-Body Dynamical Systems*, Eds. Steves, B. A., Maciejewski, A. J. and Hendry, M., 203-230, Springer Netherlands (2006).
- [29] O'Neill, B. *Semi-Riemannian Geometry*, Academic Press (1983).
- [30] Montgomery, R. and Jackman C., *No hyperbolic pants for the 4-body problem with strong potential*, Pacific Journal of Mathematics, **280**, 401 (2016).
- [31] Rajeev, S. G., *Geometry of the Motion of Ideal Fluids and Rigid Bodies*, arXiv:0906.0184 [math-ph] (2009).